



浙江大學
ZHEJIANG UNIVERSITY



Nonlinear dynamics of toroidal Alfvén eigenmodes in presence of a tearing mode

Z. W. Ma

collaborators: J. Zhu and W. Zhang

Institute for Fusion Theory and
Simulation, Zhejiang University



PPPL, 8-15-2018



浙江大學聚變理論與模擬中心 潘雲龍

Institute for Fusion Theory and Simulation, Zhejiang University



Outline

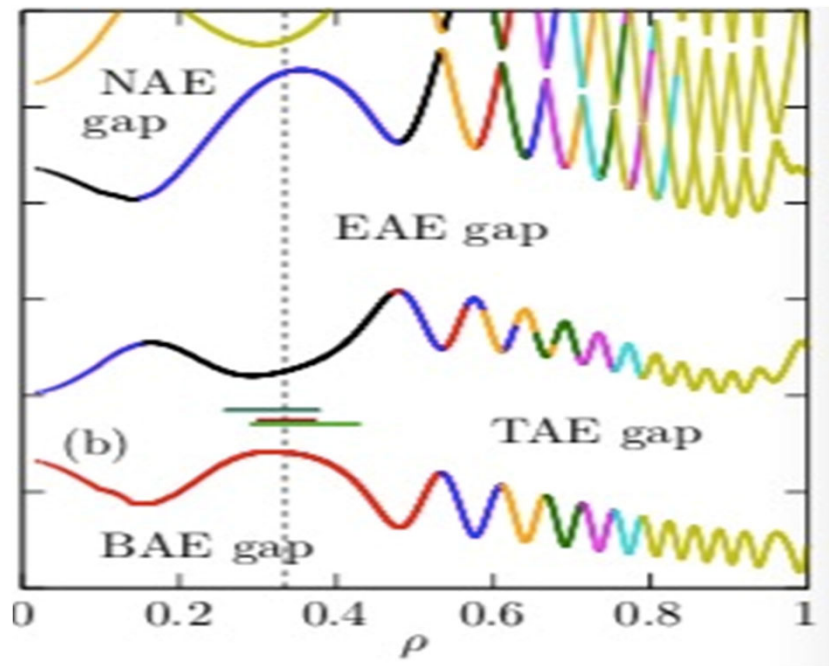
- 1. Background
- 2. A brief introduction of CLT-K code and its benchmark
- 3. Simulation results
 - a. n=2 EPM
 - b. TAE & Tearing mode
- Summary



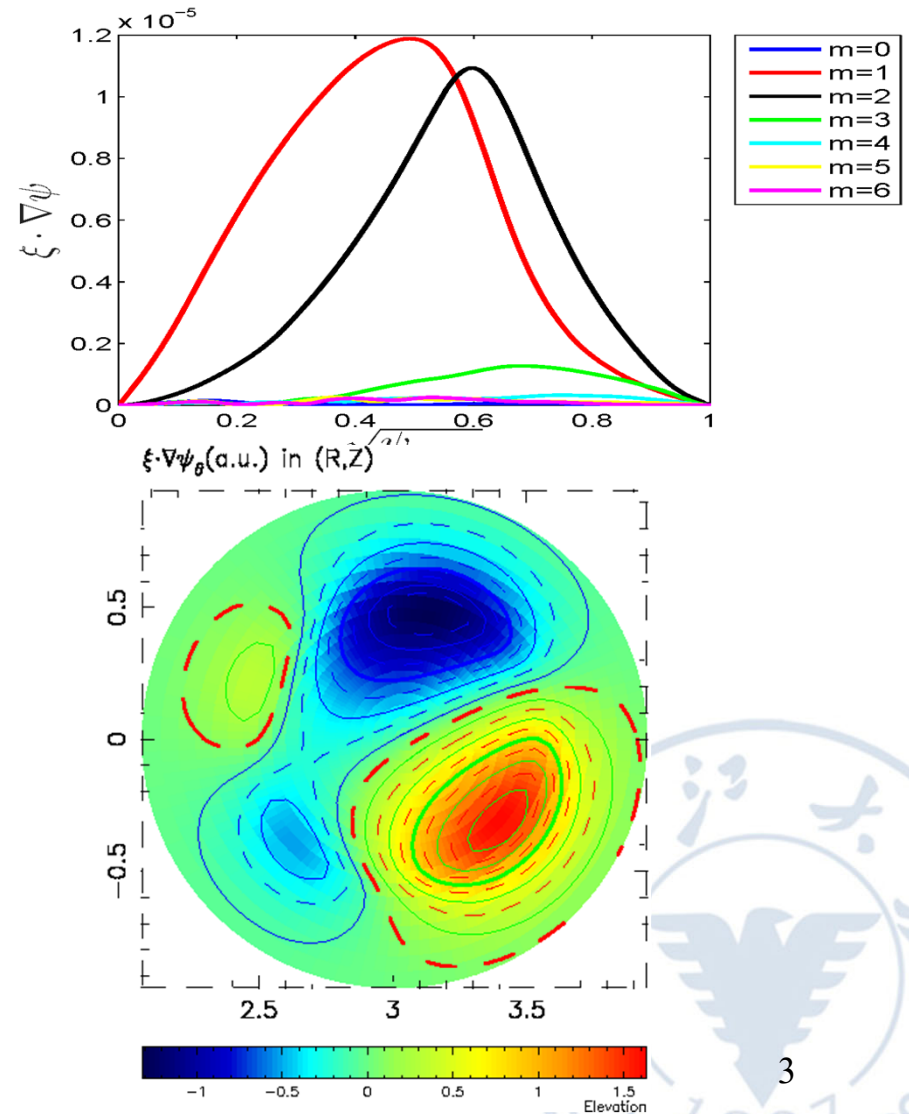
1. Background

Toroidal Alfvén eigenmodes (TAEs)

Alfvén spectrum in Tokamak



TAEs in gaps can be easily driven by energetic particles (EPs).



In DIII-D experiments, it is found that **TAE** can lead to a large percentage of EP loss!

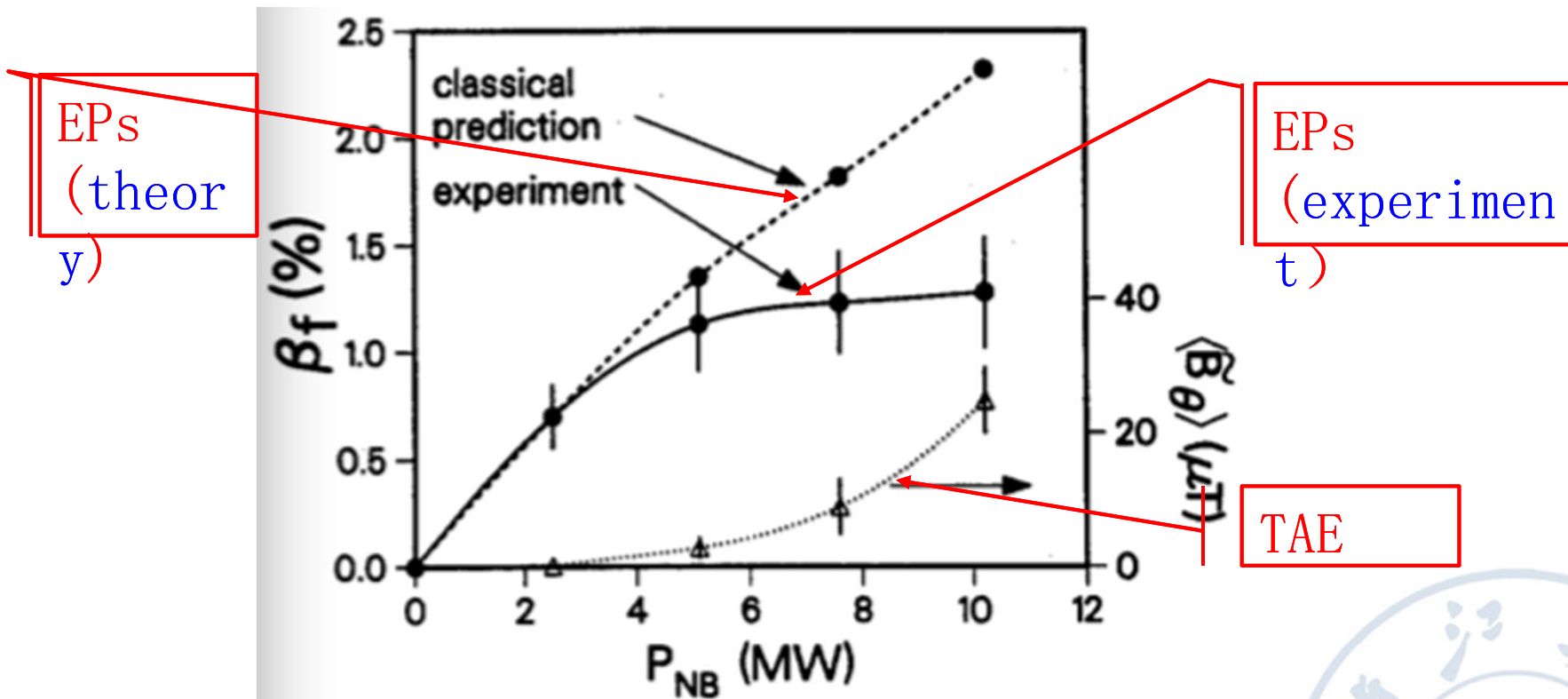


FIG. 9. Dependence of TAE activity on neutral beam power in discharge 71 524. The fast ion beta predicted by using classical

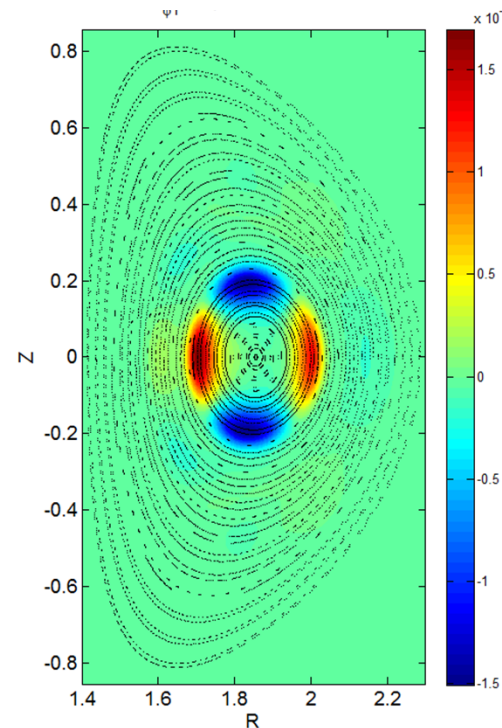
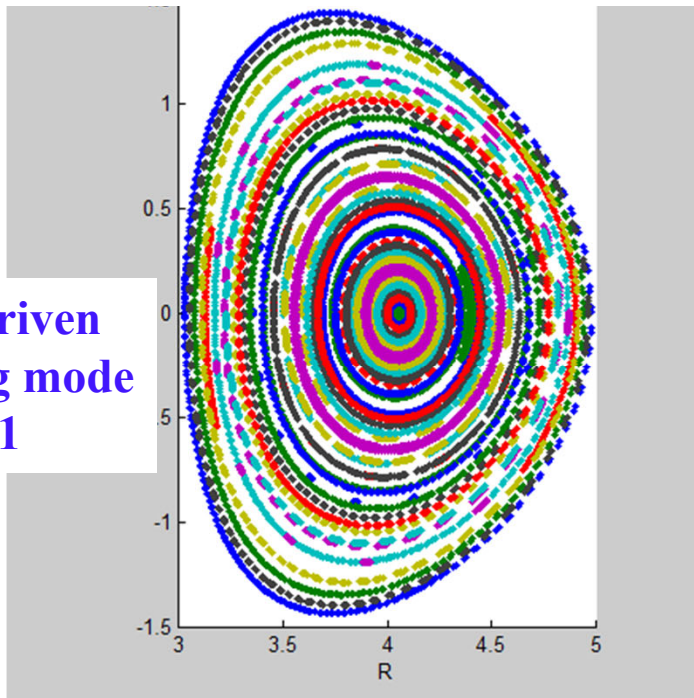
[E. Strait Nuclear Fusion
1002]



Tearing mode instability

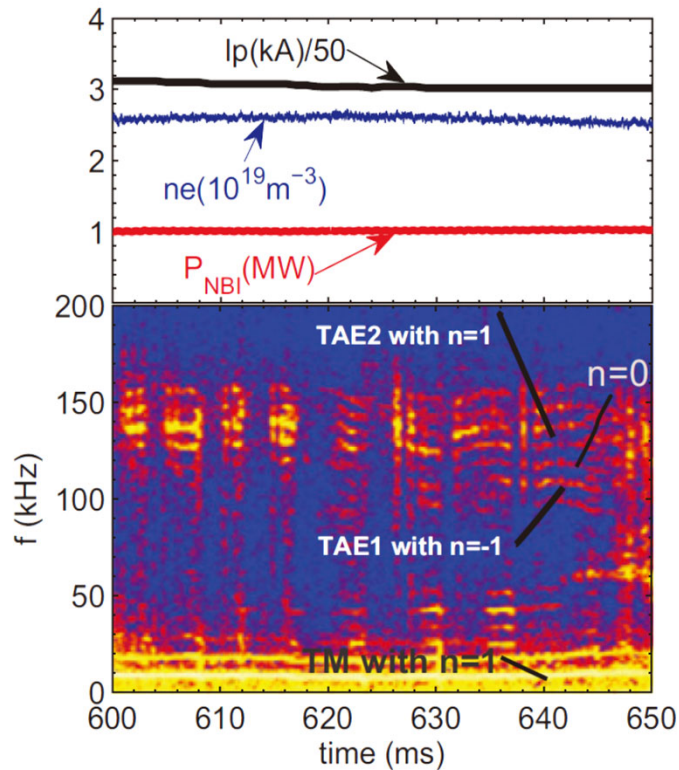
- Tearing mode instability driven by electric current is one of the most important instabilities in magnetized plasmas.
- Many eruptive phenomena in both space and laboratory are believed to be associated with the tearing mode instability.
- Tearing mode instability is regarded as the primary cause for degradation of the plasma performance in Tokamak.

Kink driven
Tearing mode
 $m/n=1/1$

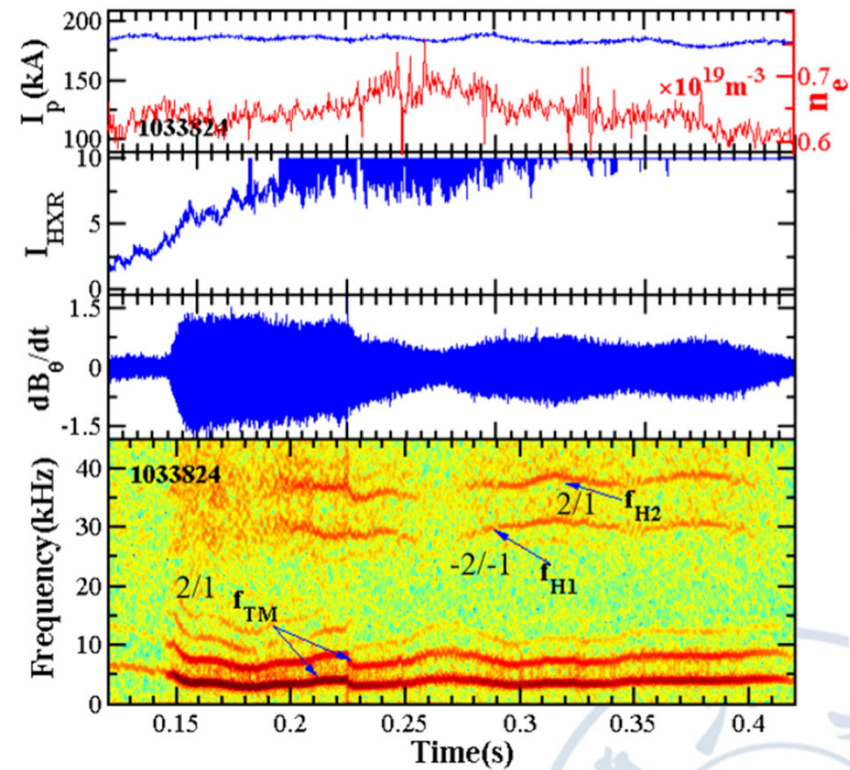


Tearing mode
 $m/n=2/1$

HL-2A



J-TEXT

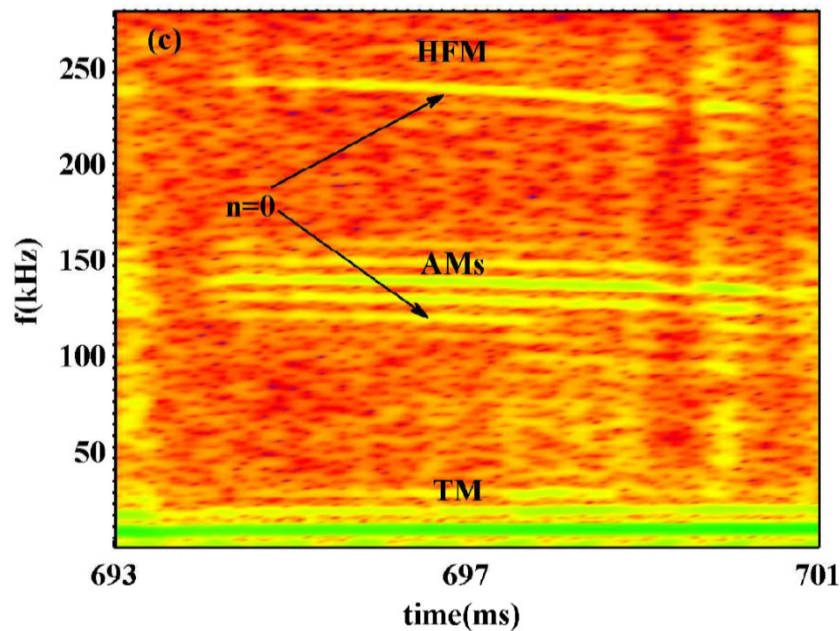


High frequency branch(TAE/BAE) and low frequency(TM) are always observed on HL-2A and J-TEXT experiments.

W. Chen *et. al.* EPL, **107** (2014) 25001

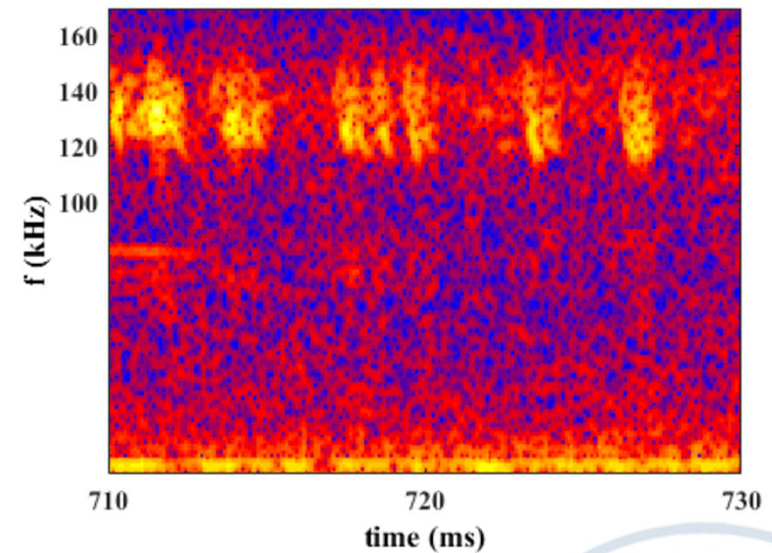
HL-2A

Weakly chirping of TAEs



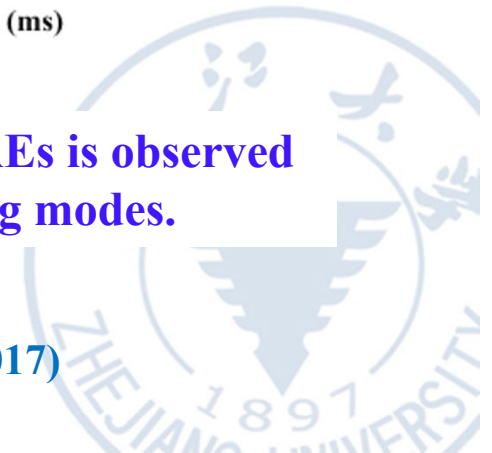
Strong TM activities lead to nonlinear mode-mode couplings and TAEs are weakly chirping.

Pitch-Fork of TAEs

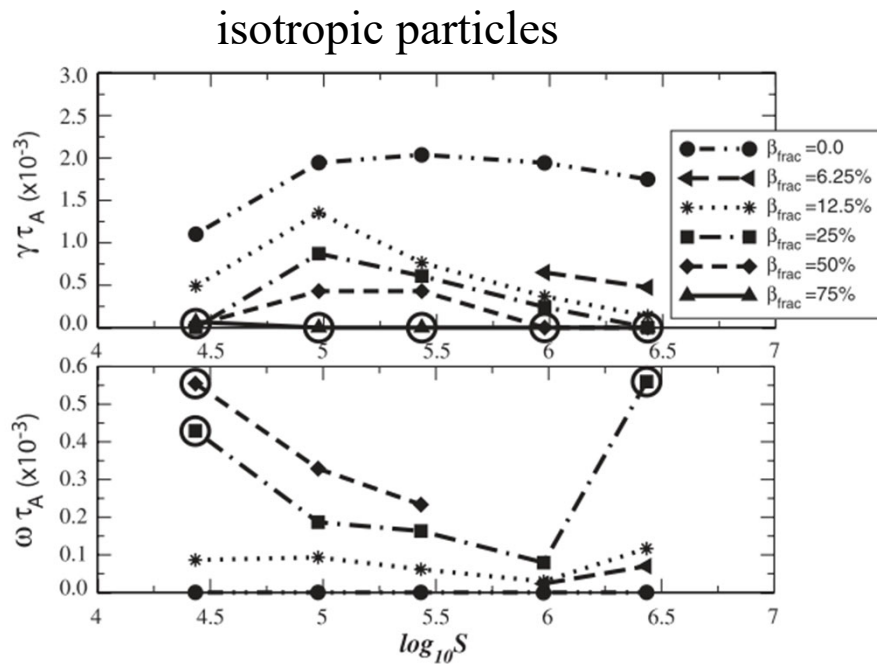


Pitch-Fork TAEs is observed without tearing modes.

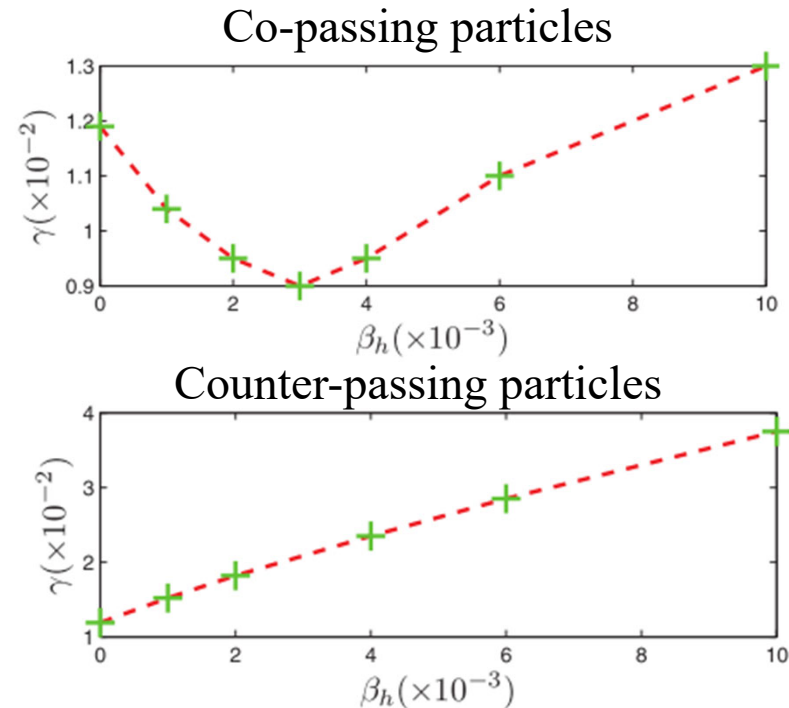
P. W. Shi *et. al. Physics of Plasmas* 24, 042509 (2017)



NIMROD (Takahashi 2009)



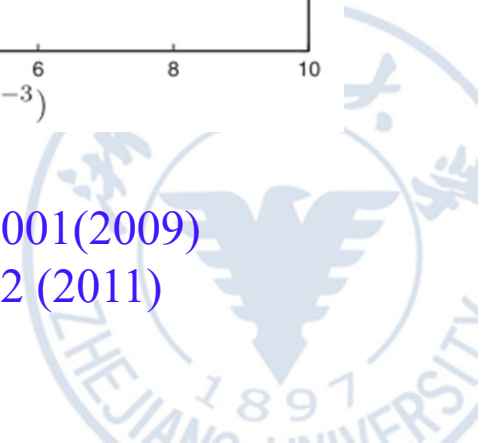
M3D-K (Cai huishan2011)



R. Takahashi, D. P. Brennan, and C. C. Kim, *Phys. Rev. Lett.* **102**, 135001(2009)

H. Cai, S. Wang, Y. Xu, J. Cao, and D. Li, *Phys. Rev. Lett.* **106**, 075002 (2011)

H. Cai and G. Y. Fu, *Phys. Plasmas* **19**, 072506 (2012).





2. A brief introduction of CLT-K code and its benchmark

The MHD component of CLT-K is based on CLT (Ci-Liu-Ti means MHD in Chinese) which is an initial value code that resolves the full set of resistive Hall MHD equations in 3D toroidal geometries.

$$\frac{\partial \rho}{\partial t} = -\nabla \cdot (\rho \mathbf{v}) + \nabla \cdot [D \nabla (\rho - \rho_0)]$$

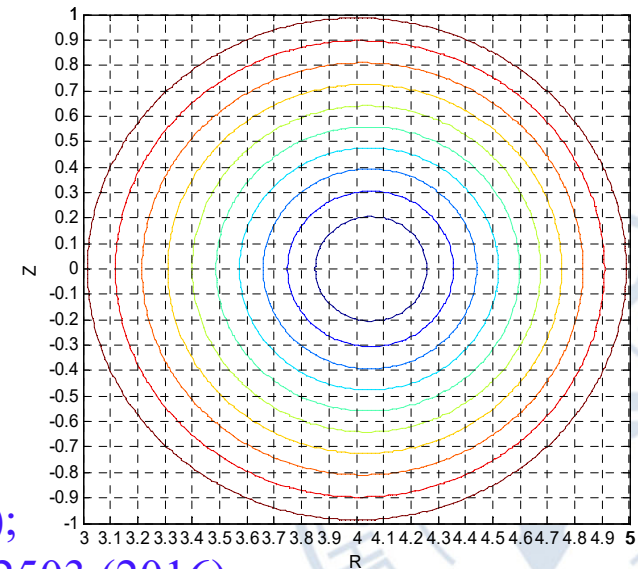
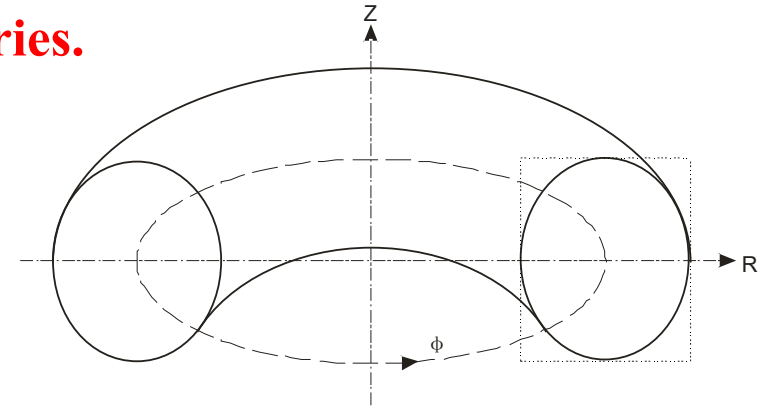
$$\frac{\partial p_e}{\partial t} = -\mathbf{v} \cdot \nabla p - \Gamma p_e \nabla \cdot \mathbf{v} + \nabla \cdot [\kappa \nabla (p - p_0)]$$

$$\frac{\partial \mathbf{v}}{\partial t} = -\mathbf{v} \cdot \nabla \mathbf{v} + (\mathbf{J} \times \mathbf{B} - \nabla p_e) / \rho + \nabla \cdot [\nu \nabla (\mathbf{v} - \mathbf{v}_0)]$$

$$\frac{\partial \mathbf{B}}{\partial t} = -\nabla \times \mathbf{E}$$

$$\mathbf{E} = -\mathbf{v} \times \mathbf{B} + \eta (\mathbf{J} - \mathbf{J}_0) + \frac{1}{ne} (\mathbf{J} \times \mathbf{B} - \nabla p_e)$$

$$\mathbf{J} = \nabla \times \mathbf{B}$$



S. Wang and Z. W. Ma, *Phys. Plasmas* **22**, 122504 (2015);

S. Wang, Z. W. Ma, and W. Zhang, *Phys. Plasmas* **23**, 052503 (2016)



The Hybrid Kinetic-MHD Equations

$$\frac{\partial \rho}{\partial t} = -\nabla \cdot (\rho \mathbf{v}) + \nabla \cdot [D \nabla (\rho - \rho_0)]$$

$$\frac{\partial p_e}{\partial t} = -\mathbf{v} \cdot \nabla p - \Gamma p_e \nabla \cdot \mathbf{v} + \nabla \cdot [\kappa \nabla (p - p_0)]$$

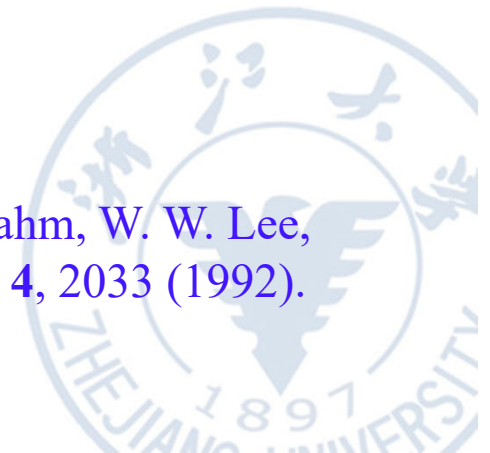
$$\frac{\partial \mathbf{v}}{\partial t} = -\mathbf{v} \cdot \nabla \mathbf{v} + [(\mathbf{J} - \mathbf{J}_E) \times \mathbf{B} - \nabla p_e] / \rho + \nabla \cdot [\nu \nabla (\mathbf{v} - \mathbf{v}_0)]$$

$$\frac{\partial \mathbf{B}}{\partial t} = -\nabla \times \mathbf{E}$$

$$\mathbf{E} = -\mathbf{v} \times \mathbf{B} + \eta (\mathbf{J} - \mathbf{J}_0) + \frac{1}{ne} (\mathbf{J} \times \mathbf{B} - \nabla p_e)$$

$$\mathbf{J} = \nabla \times \mathbf{B}$$

W. Park, S. Parker, H. Biglari, M. Chance, L. Chen, C. Z. Cheng, T. S. Hahm, W. W. Lee, R. Kulsrud, D. Monticello, L. Sugiyama, and R. B. White, *Phys. Fluids B* 4, 2033 (1992).





Drift kinetic equations for energetic particles

$$\frac{d\mathbf{X}}{dt} = \frac{1}{B_{\parallel}^*} [v_{\parallel} \mathbf{B}^* + \mathbf{E}^* \times \mathbf{b}]$$

Cary 2009

$$\frac{dv_{\parallel}}{dt} = \frac{Z_h e}{m B_{\parallel}^*} \mathbf{B}^* \cdot \mathbf{E}^*$$

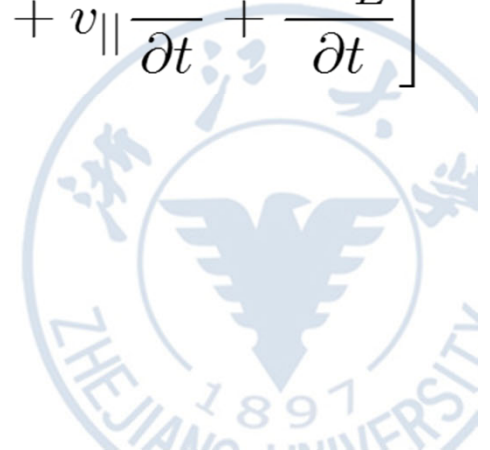
where

$$\mathbf{B}^* = \mathbf{B} + \frac{mv_{\parallel}}{Z_h e} \nabla \times \mathbf{b} + \frac{m}{Z_h e} \nabla \times \mathbf{v}_E \quad B_{\parallel}^* = \mathbf{B}^* \cdot \mathbf{b}$$

$$\mathbf{E}^* = -\nabla \Phi^* - \frac{\partial \mathbf{A}^*}{\partial t} = \mathbf{E} - \frac{m}{Z_h e} \left[\frac{1}{m} \mu \nabla B + \frac{1}{2} \nabla |\mathbf{v}_E|^2 + v_{\parallel} \frac{\partial \mathbf{b}}{\partial t} + \frac{\partial \mathbf{v}_E}{\partial t} \right]$$

$$\mathbf{v}_E = \frac{\mathbf{E} \times \mathbf{B}}{B^2}$$

J. R. Cary and A. J. Brizard, Rev. Mod. Phys. 81, 693 (2009).





Current \mathbf{J}_E from energetic particles

$$\begin{aligned} \mathbf{J}_E &= \mathbf{J}_{GC} + \mathbf{J}_{MAG} + \mathbf{J}_{POL} \\ &= \int Z_h e (\mathbf{v}_{\text{curvature}} + \mathbf{v}_{\nabla B} + \mathbf{v}_B + \mathbf{v}_{EB}) f(\mathbf{v}) d\mathbf{v} \\ &\quad - \nabla \times \int \mu \mathbf{b} f(\mathbf{v}) d\mathbf{v} + \int Z_h e \mathbf{v}_{\text{polarization}} f(\mathbf{v}) d\mathbf{v}. \end{aligned}$$

$$\mathbf{v}_{\text{curvature}} = \frac{mv_{\parallel}^2}{Z_h e B_{\parallel}^*} \nabla \times \mathbf{b}$$

$$\mathbf{v}_{\text{polarization}} = \frac{m}{Z_h e B_{\parallel}^*} \mathbf{b} \times \frac{\partial \mathbf{v}_E}{\partial t}$$

$$\mathbf{v}_{\nabla B} = \frac{\mu}{Z_h e B_{\parallel}^*} \mathbf{b} \times \nabla B$$

\mathbf{J}_{GC} : Guiding center current

$$\mathbf{v}_B = v_{\parallel} \frac{\mathbf{B}}{B_{\parallel}^*}$$

\mathbf{J}_{MAG} : Magnetization current

\mathbf{J}_{POL} : Polarization current

$$\mathbf{v}_{EB} = \frac{m}{Z_h e B_{\parallel}^*} \left[v_{\parallel} \nabla \times \mathbf{v}_E + \frac{1}{2} \mathbf{b} \times \nabla |\mathbf{v}_E|^2 \right]$$





Benchmark for CLT-K

Parameters for n=1 TAE benchmark study

- **Equilibrium parameters**

$$n = 1, R_0/a = 3, q = 1.1 + \Psi, \langle \beta_{\text{total}} \rangle = 0.5\%$$

- **Hot particle parameters**

$$v_0/v_A = 1.7, \rho_h/a = 0.085, \langle \beta_h \rangle_{\text{av}} = 0.4\%$$

- **Slowing down distribution**

$$f_0(P_\phi, E, \Lambda) = \frac{1}{v^3 + v_c^3} \left[1 + \text{erf} \left(\frac{v_0 - v}{0.2v_A} \right) \right] \exp \left(-\frac{\langle \psi \rangle}{0.37\Delta\psi} \right)$$

- **For simplify**

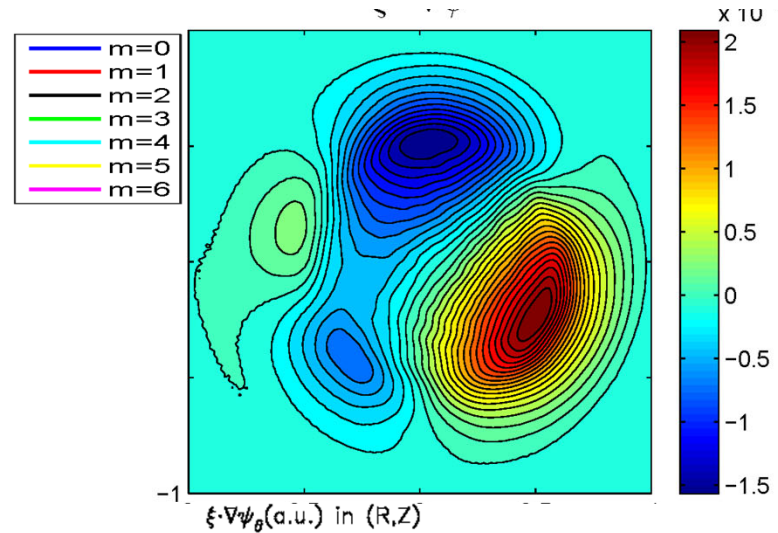
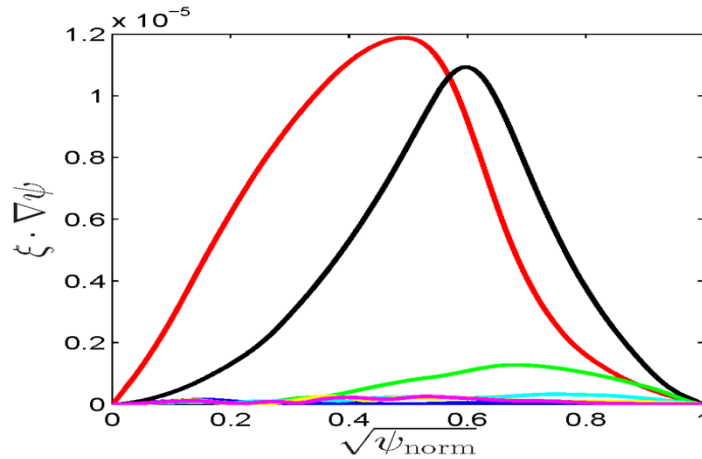
$$\langle \psi \rangle = -P_\phi/Z_h e + \frac{m}{Z_h e} \left\langle v_{\parallel} R \frac{B_\phi}{B} \right\rangle \approx -P_\phi/Z_h e$$



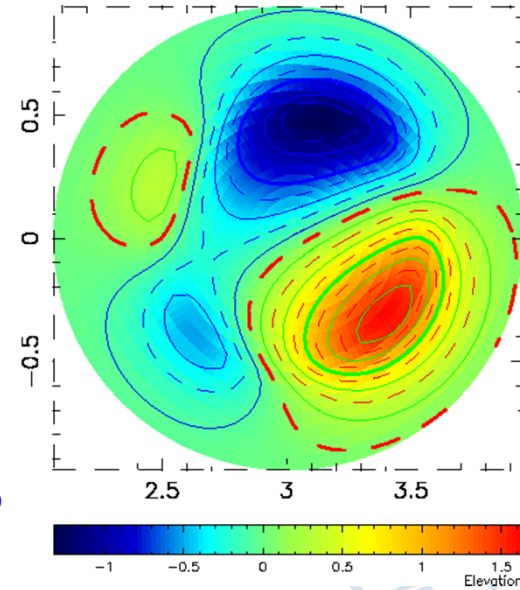
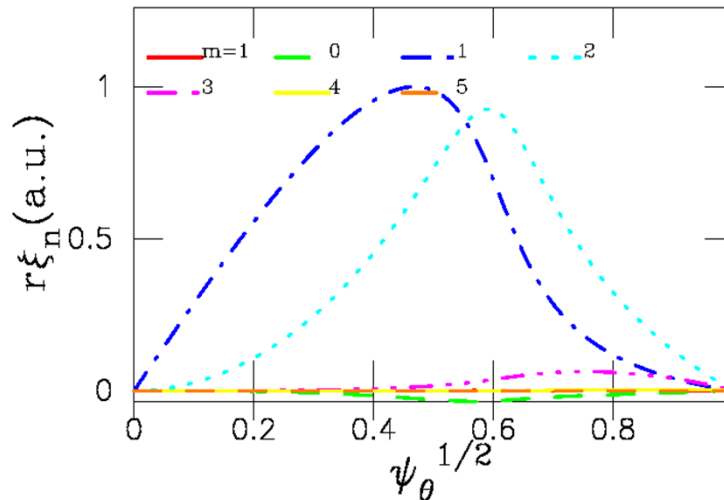


Benchmark study on linear n=1 TAE

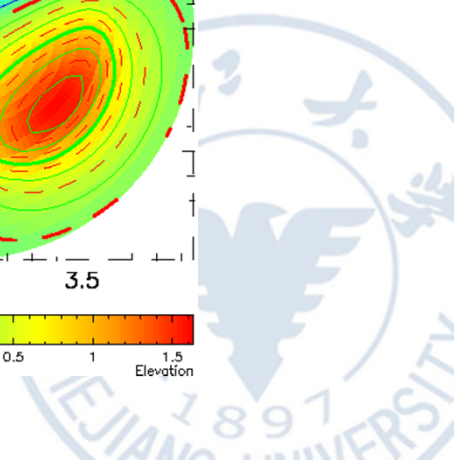
CLT-K



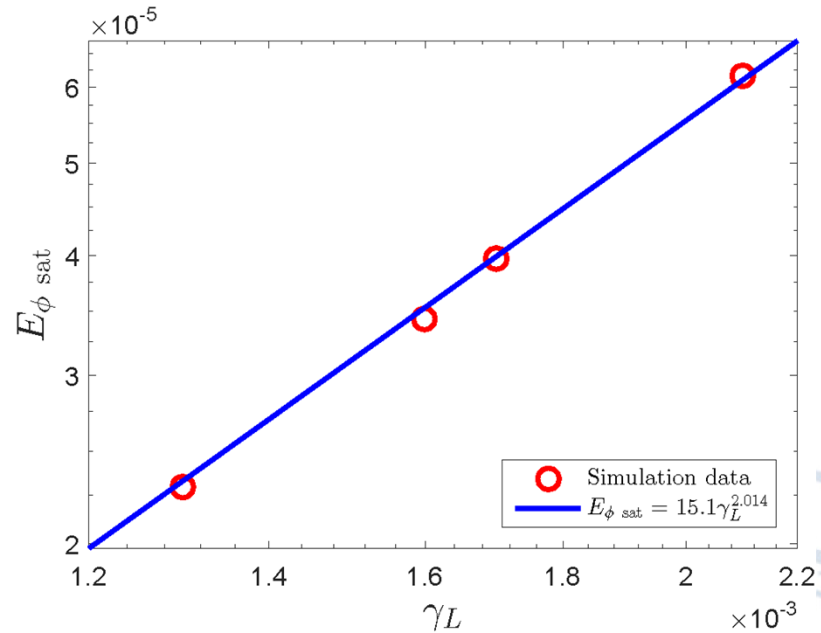
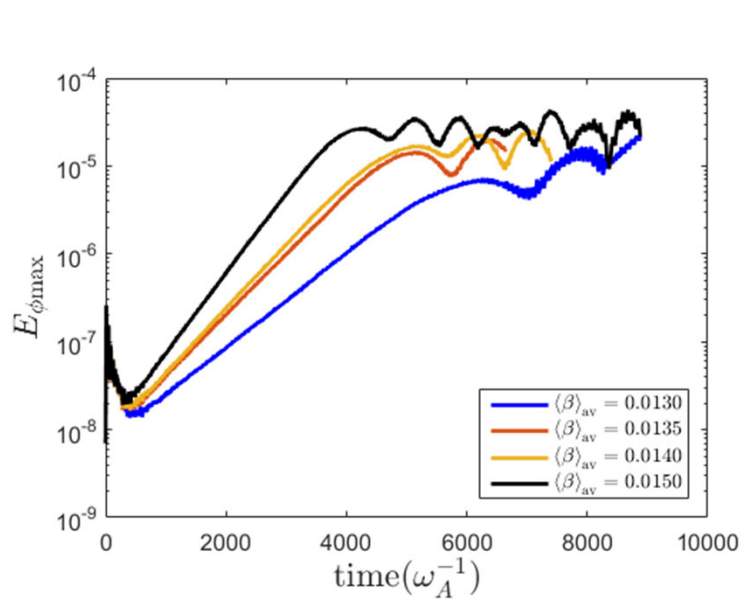
NOVA



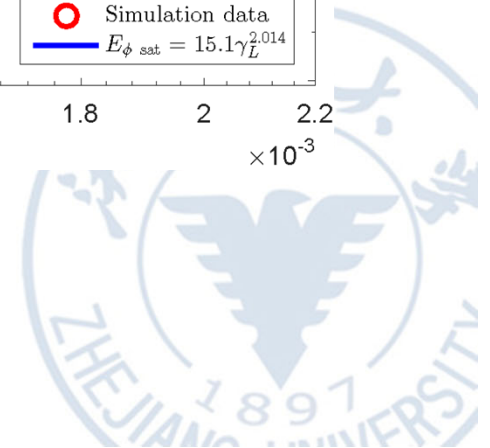
TAE : $\omega_{\text{NOVA}}=0.100$ $\omega_{\text{antenna}}=0.097$ $\omega_{\text{EP}}=0.093$
 $\gamma/\omega\beta_{\text{NOVA}}=1$ $\gamma/\omega\beta_{\text{EP}}=1.25$



Benchmark study on nonlinear n=1 TAE



Theoretical scaling law: $E_{\phi \text{ sat}} \sim \gamma_L^{2.014}$!



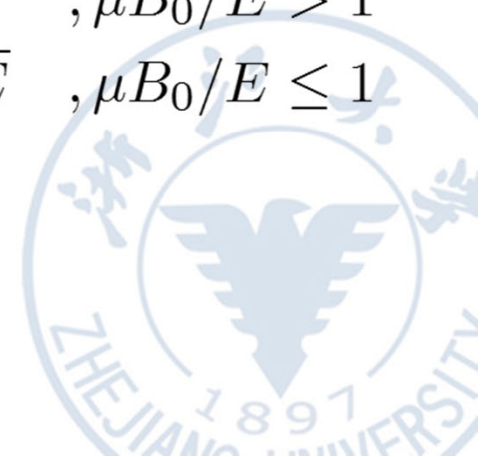
3. Simulation results

a. n=2 EPM (PoP,2016)

Parameters for n=2 EPM simulation

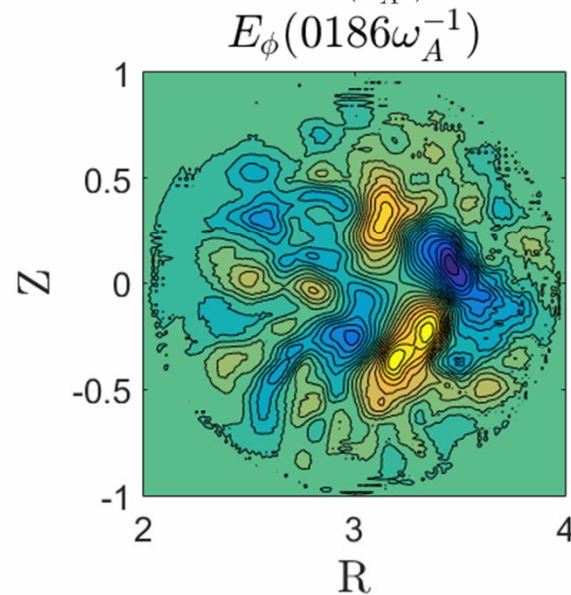
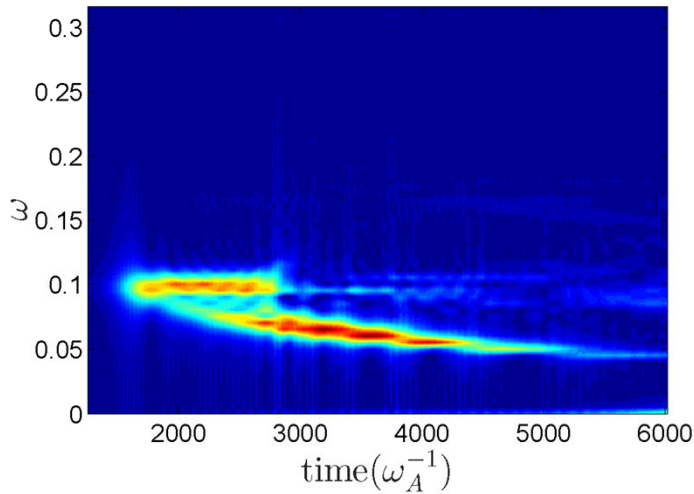
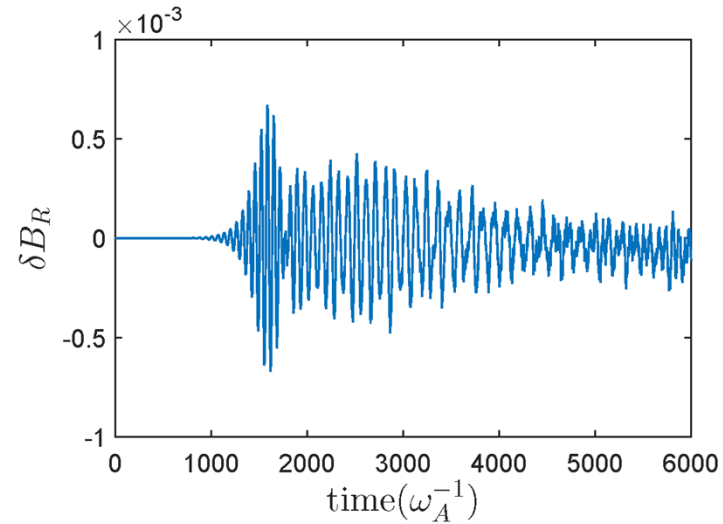
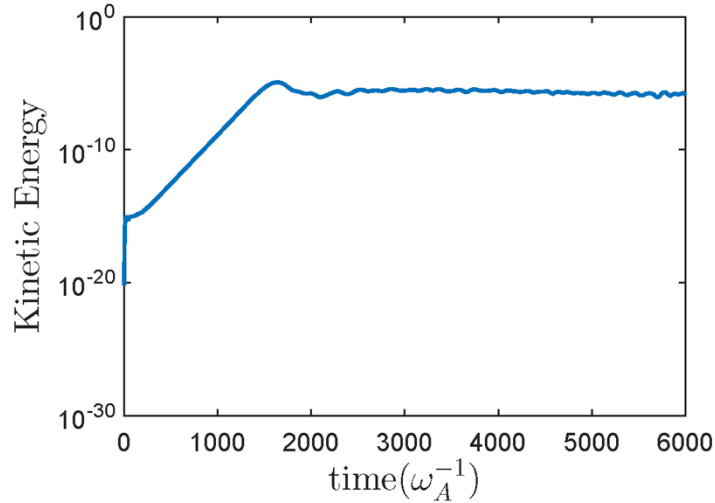
- $n=2$
- $q_0 = 1.25$
- $\text{Beta}_{av} = 0.016$

$$\langle \psi \rangle = \begin{cases} -P_\phi / (Z_h e) & , \mu B_0 / E > 1 \\ -P_\phi / (Z_h e) + \frac{m}{Z_h e} \text{sgn}(v_{\parallel}) v R_0 \sqrt{1 - \mu B_0 / E} & , \mu B_0 / E \leq 1 \end{cases}$$

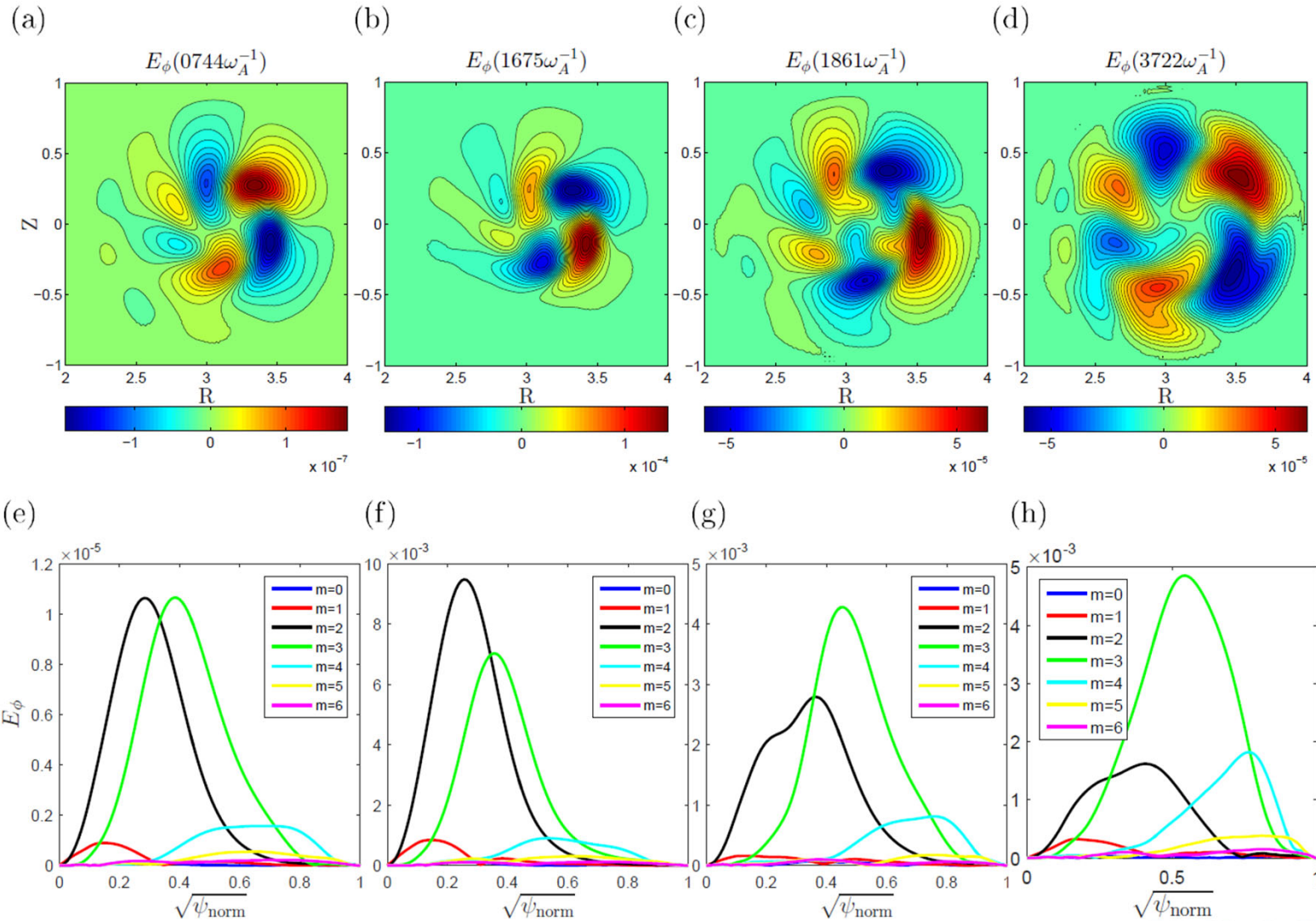




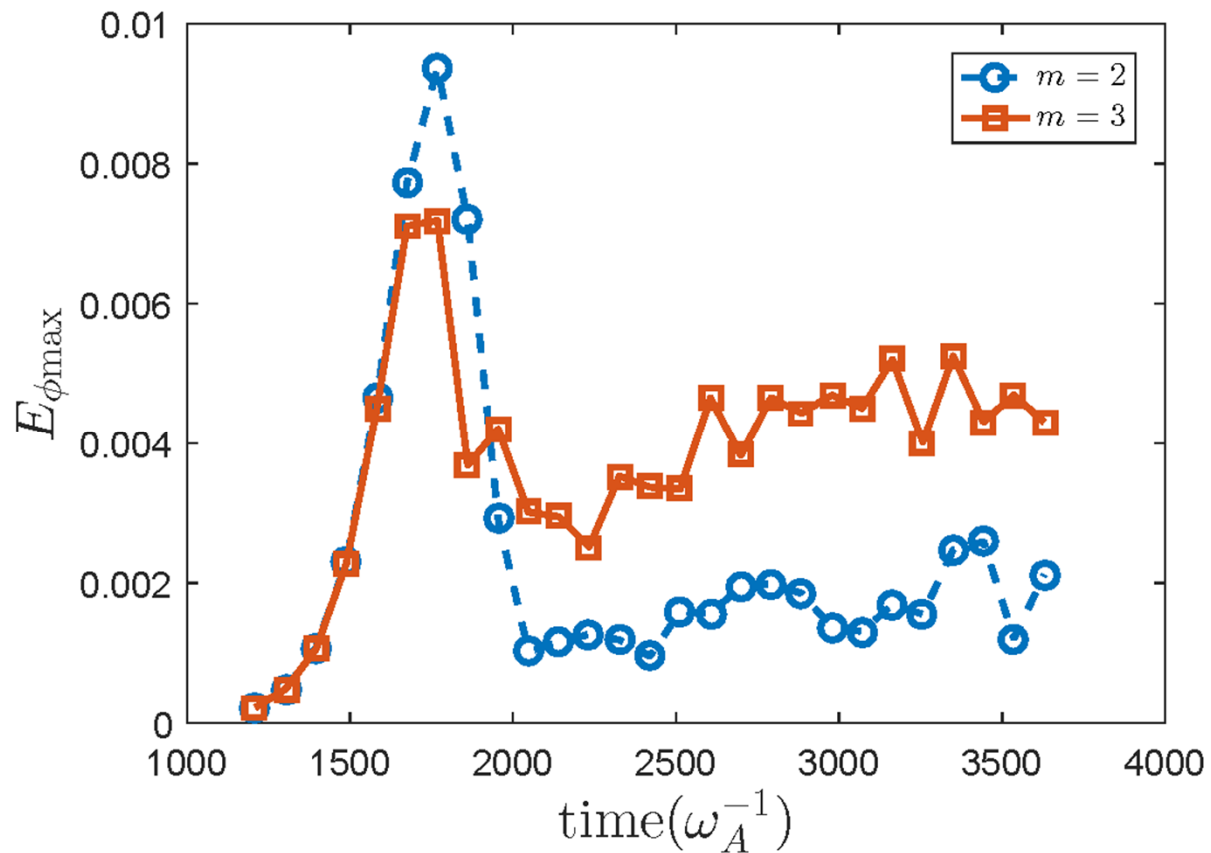
Time evolution of frequency $n=2$ mode driven by isotropic energetic particles



Time evolution of mode structure for n=2 mode



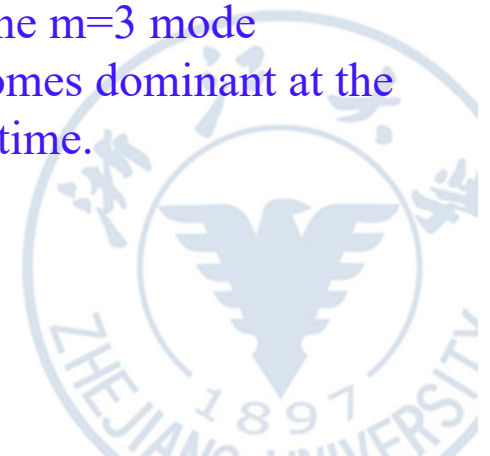
Time evolutions of peak values for two poloidal harmonics (m=2 and 3)



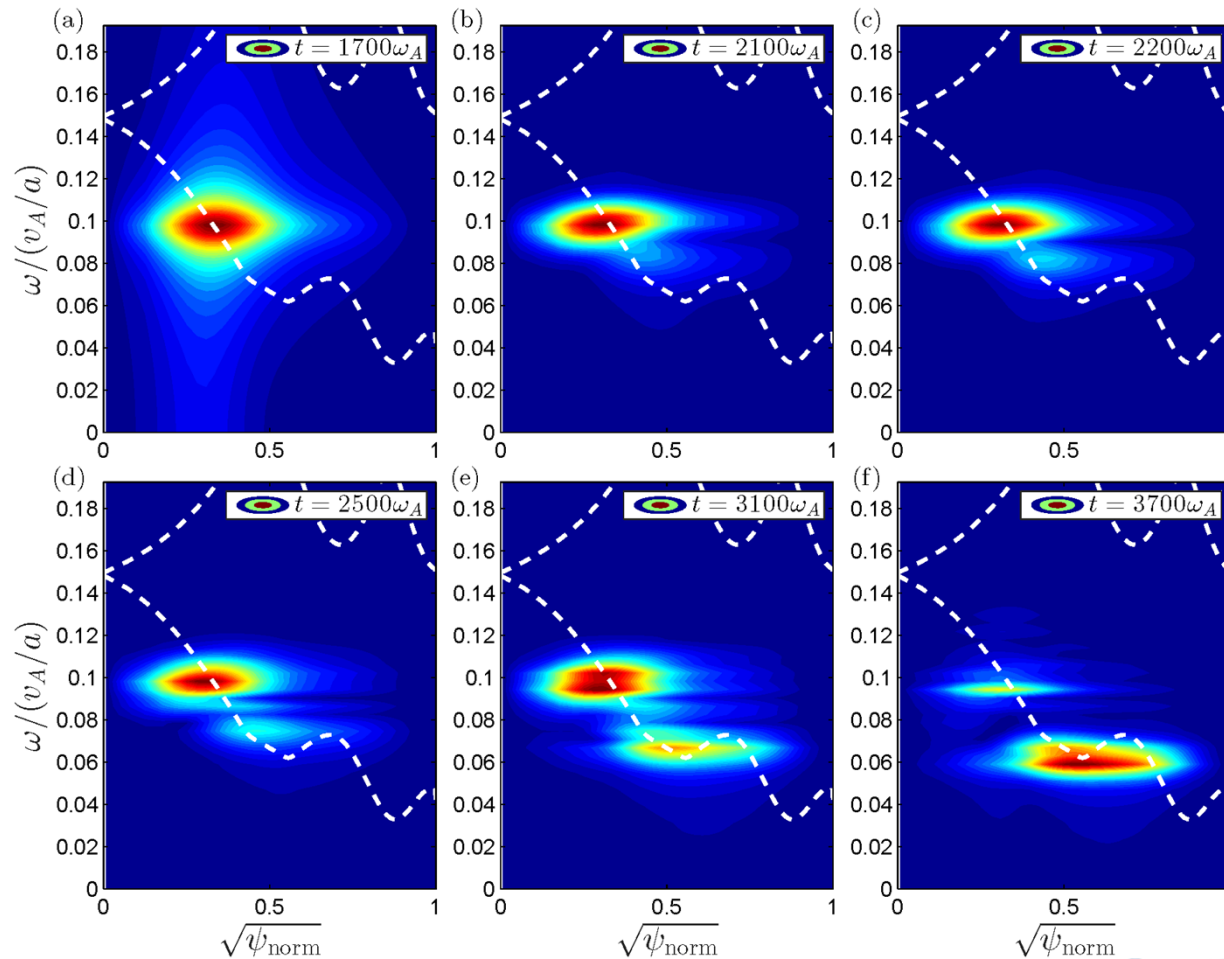
1. m=2 and m=3 modes are almost the same during the linear stage, which is TAE-like structure.

2. The m=2 mode is overtaken than the m=3 mode for a short period.

3. The m=3 mode becomes dominant at the late time.



Mode power structure

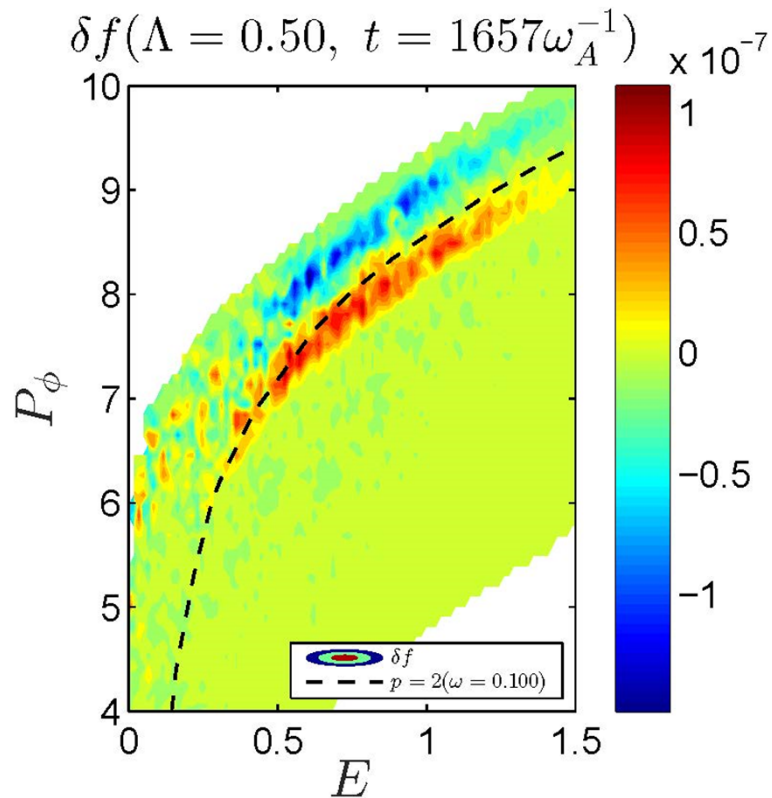


EPM (initially TAE-like or rTAE) is linearly unstable and one component of EPM remains the frequency unchanged while another component of EPM chirps down to a BAE gap during the nonlinear phase, which can be called BAE-like EPM.

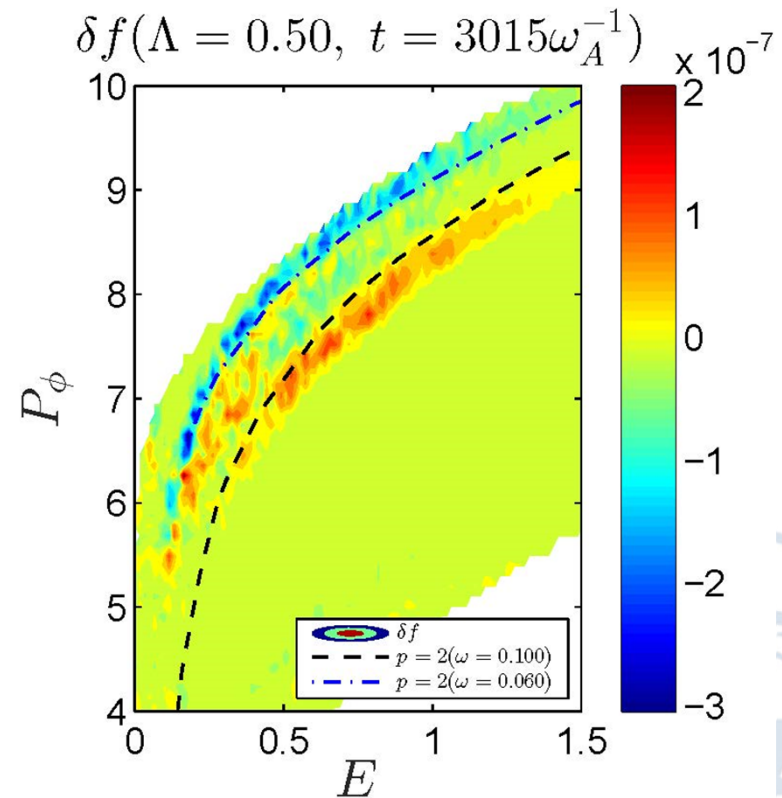
Comparisons of δf for $\Lambda=0.50$

resonant line along a constant phase : $\dot{\Theta} \equiv n\omega_\phi - p\omega_\theta - \omega = 0$

Linear stage



Nonlinear stage



The same movement is also observed for $\Lambda=0.00, 0.25$ cases, but it is more evident for $\Lambda=0.50$ cases

b. n=1 TAE and tearing mode NF,2018

- **Equilibrium parameters**

$$R_0=4\text{m}, a=1\text{m}, \beta_{\text{thermal}}=0, \eta=10^{-5\sim-7}$$

- **Hot particle parameters**

$$v_0/v_A = 1.7, \rho_h/a = 0.085, \langle \beta_h \rangle_{\text{av}} = \mathbf{1.6\%}$$

- **Slowing down distribution**

$$f_0(P_\phi, E, \Lambda) = \frac{1}{v^3 + v_c^3} \left[1 + \text{erf} \left(\frac{v_0 - v}{0.2v_A} \right) \right] \exp \left(-\frac{\langle \psi \rangle}{0.37\Delta\psi} \right)$$

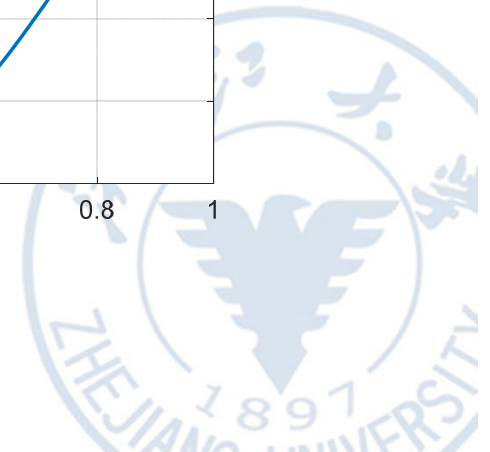
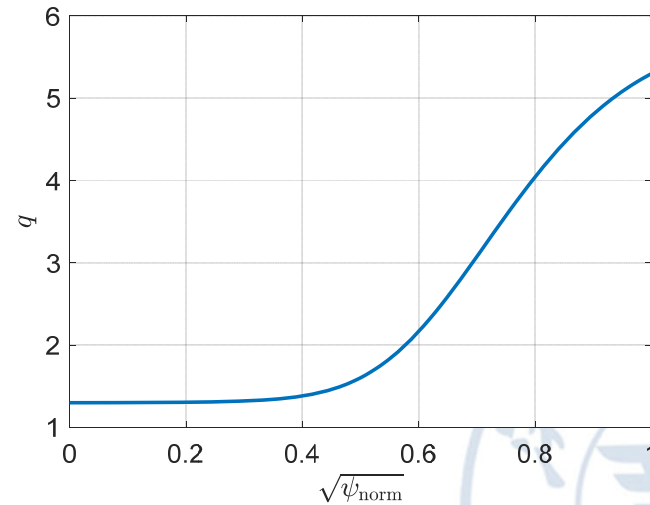
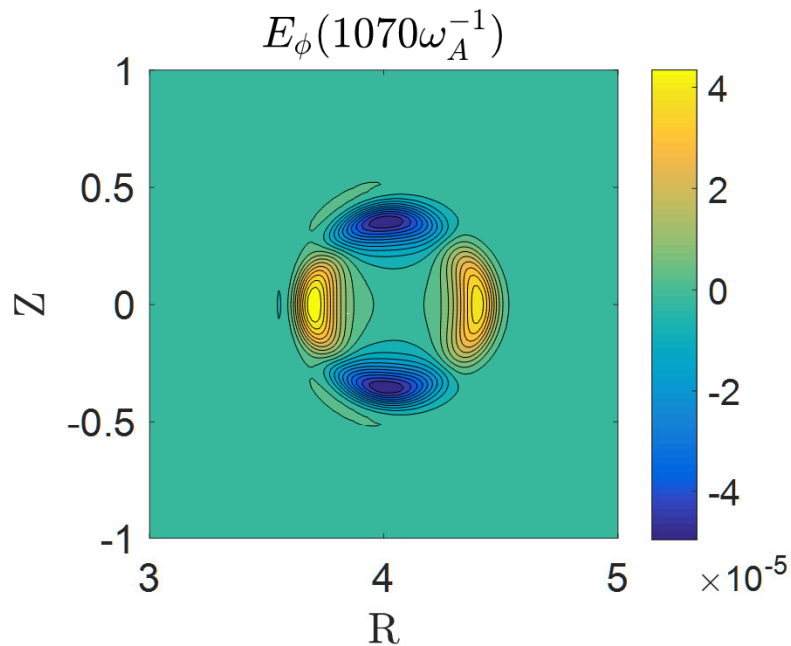
- **For simplify**

$$\langle \psi \rangle = \begin{cases} -P_\phi/(Z_h e) & , \mu B_0/E > 1 \\ -P_\phi/(Z_h e) + \frac{m}{Z_h e} \text{sgn}(v_{\parallel}) v R_0 \sqrt{1 - \mu B_0/E} & , \mu B_0/E \leq 1 \end{cases}$$

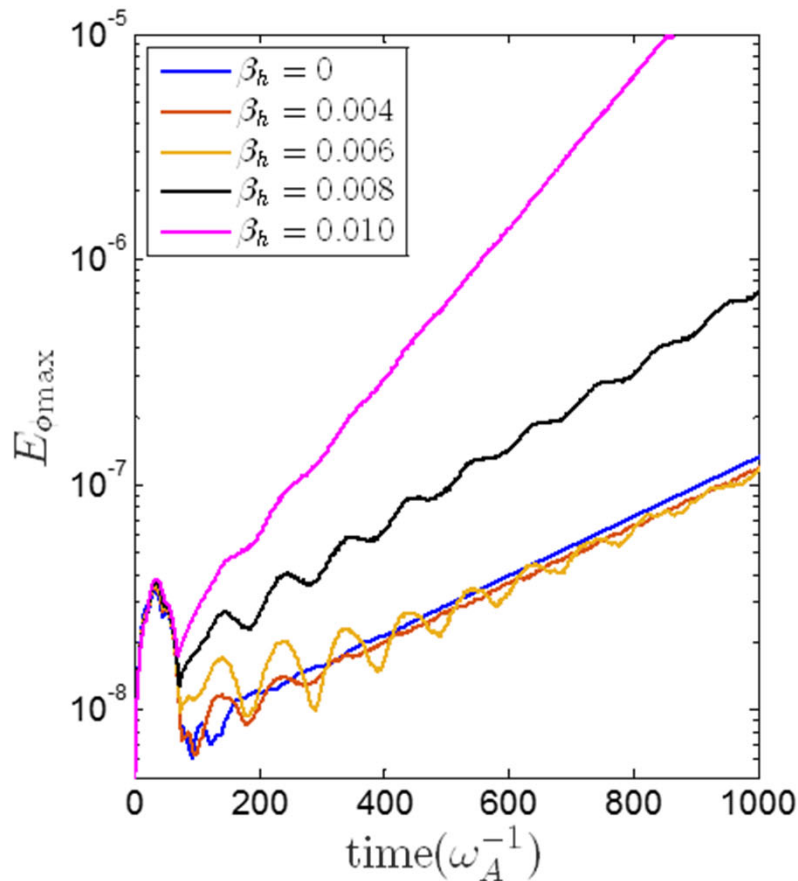


Assumption:

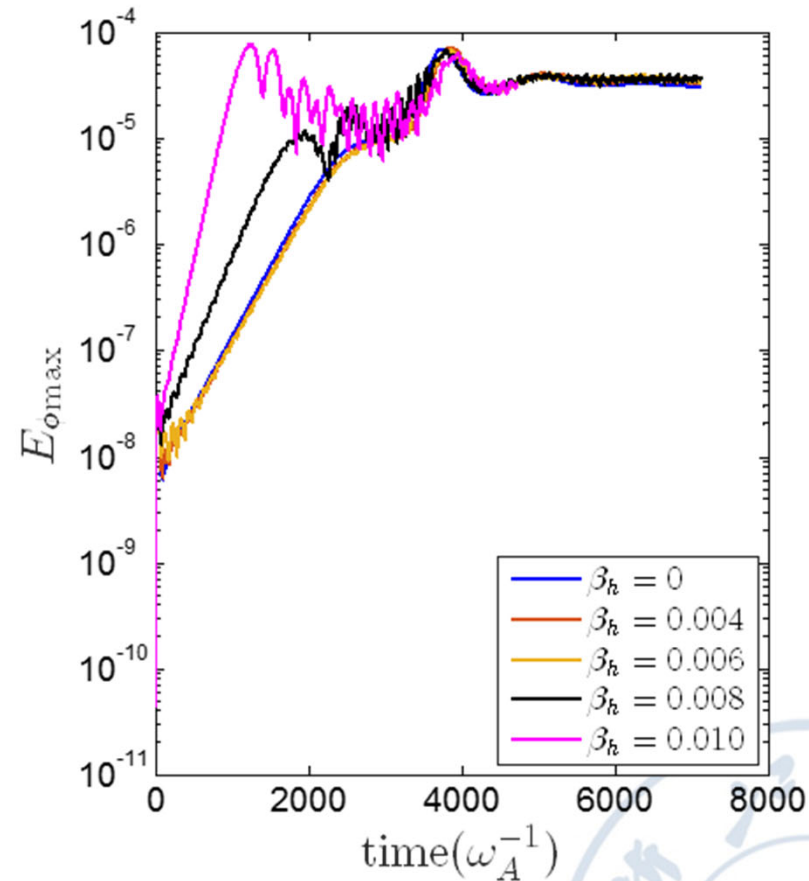
- 1. The effect of fast ions on the equilibrium are neglected.
- 2. Only $n=1$ component for \mathbf{J}_h is considered.



Time evolution of the mode with different β_h

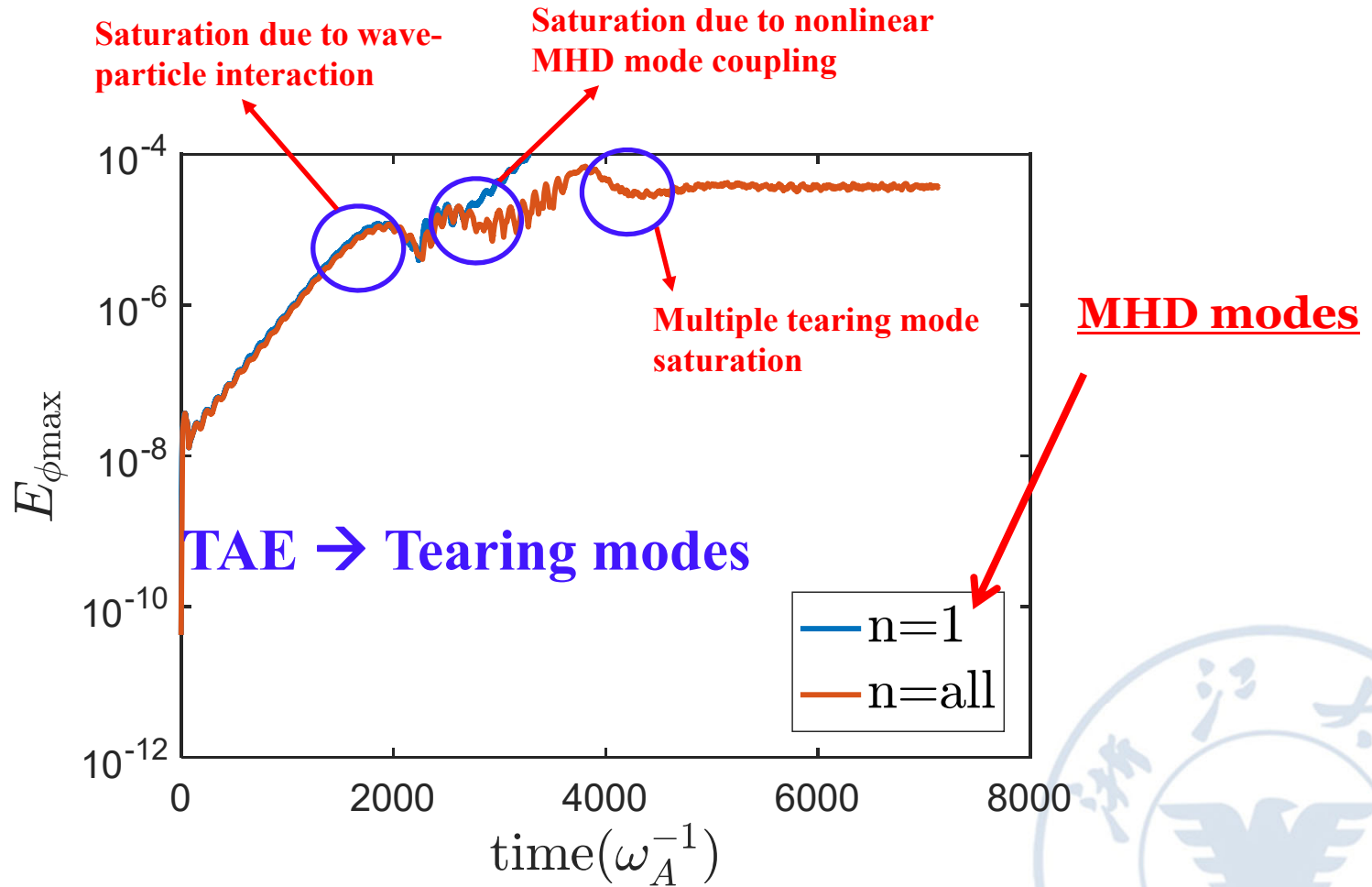


For small β_h : weakly stabilization effect
 For large β_h : destabilization effect

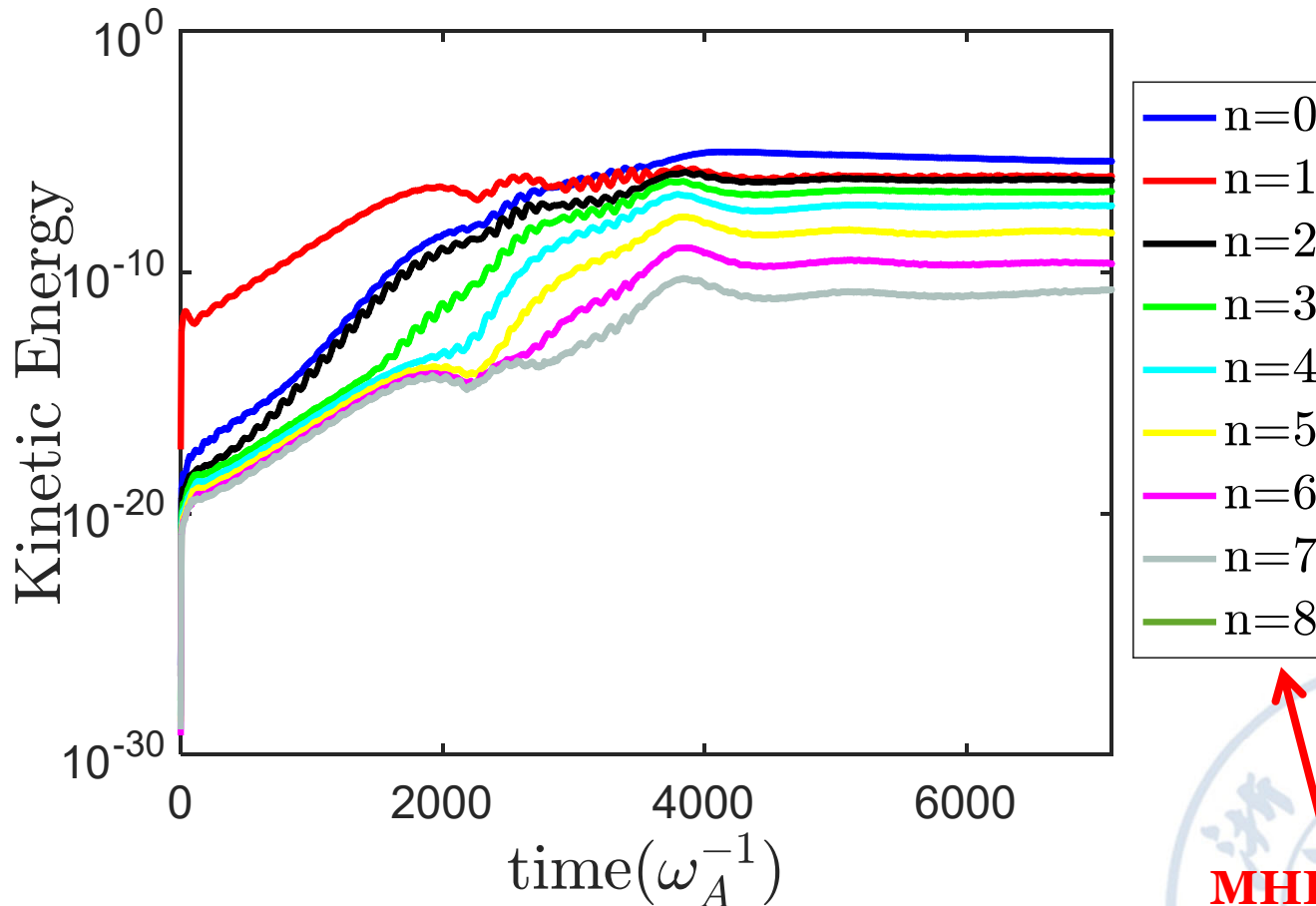


Final nonlinear saturation levels are almost same.

Time evolution of the mode ($\beta_h = 0.008$)



Time evolution of different components of mode

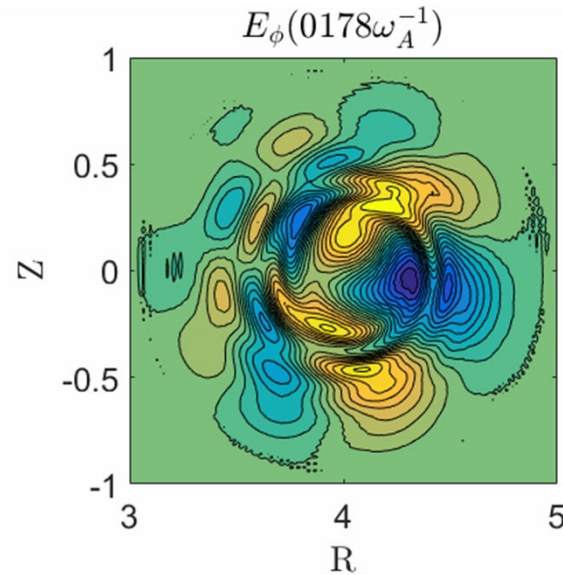
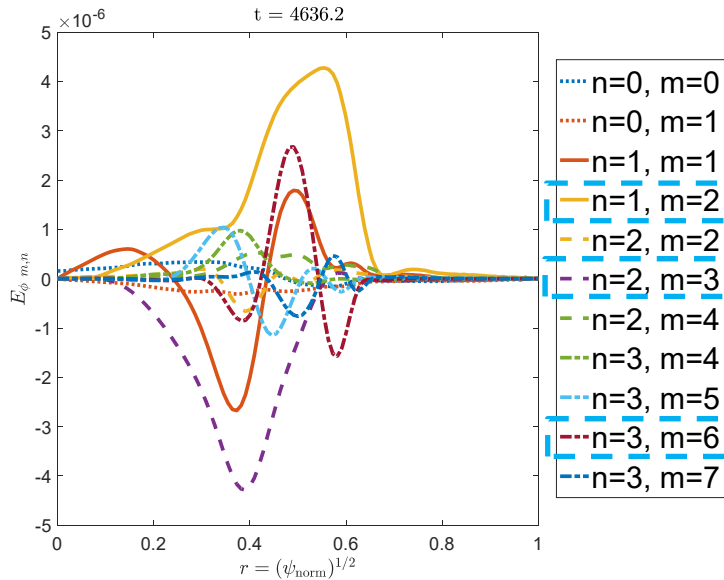
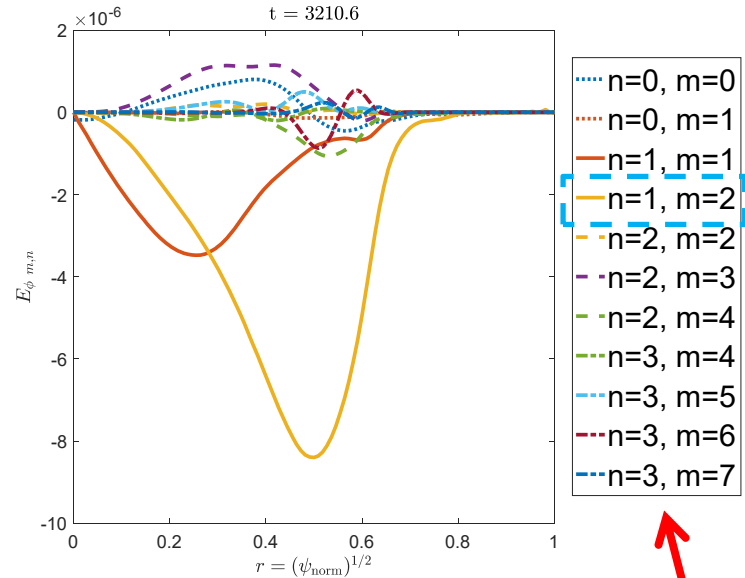
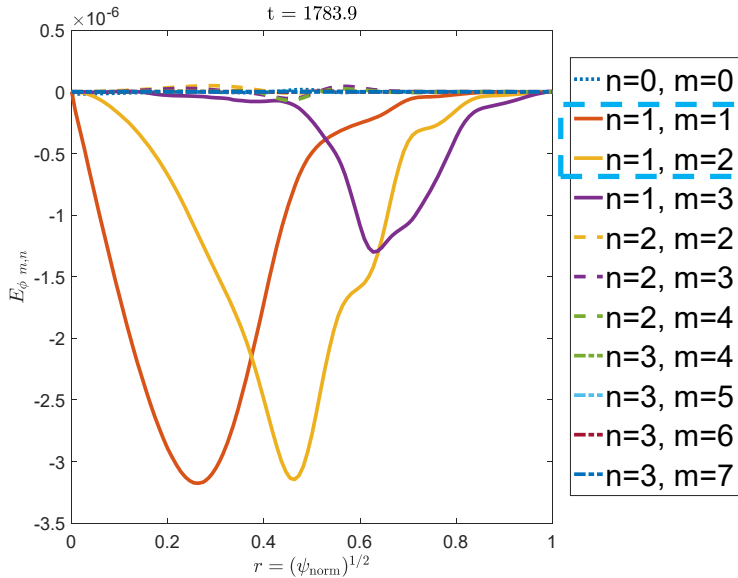


MHD modes

1. Beating mode: $\gamma_{n=0} = \gamma_{n=2} = 2\gamma_{n=1}$
2. Oscillatory behavior: $\omega = \omega_{TAE} - \omega_{TM}$



Snapshots of the mode structure



MHD modes

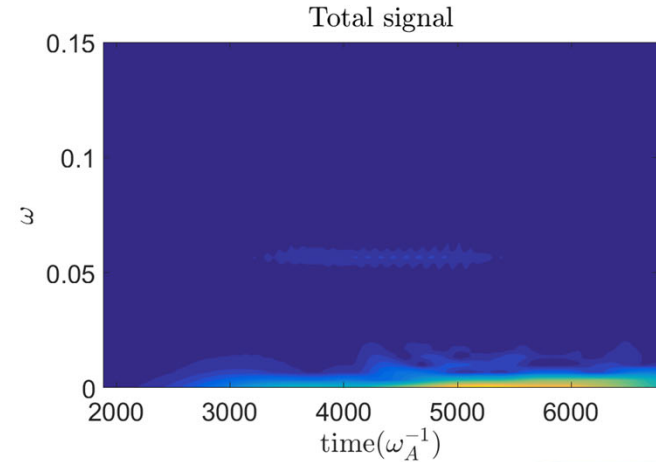
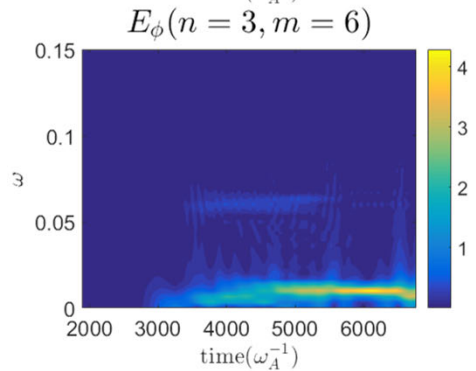
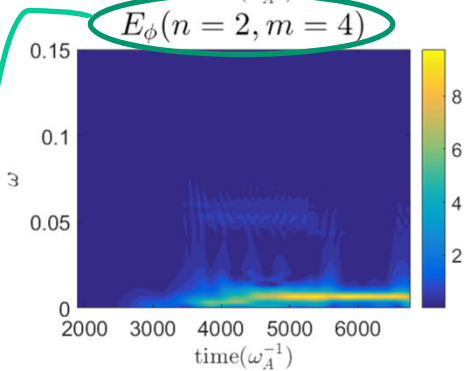
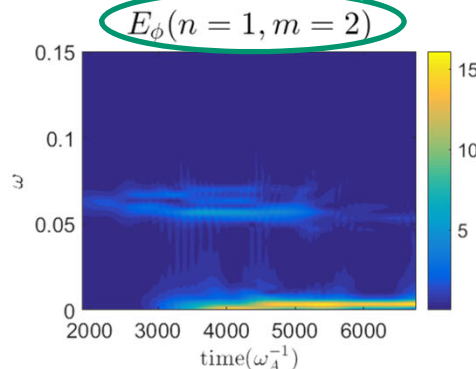
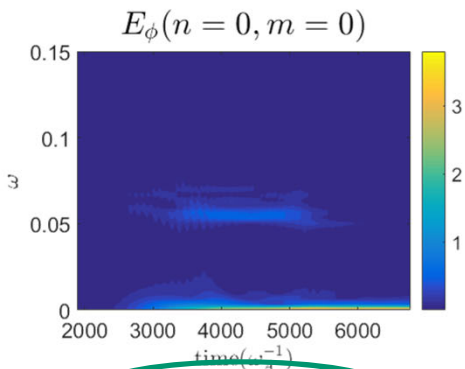




Evolution of power spectrum for different mode

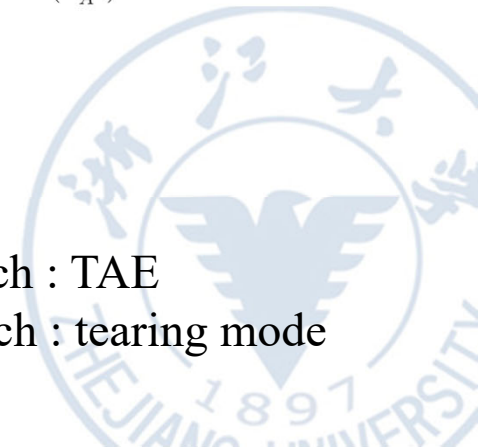
n=1 TAE is dominant at the linear stage, then other TAEs (n=0,2,3) are excited during the nonlinear stage.

Primary mode



Secondary mode

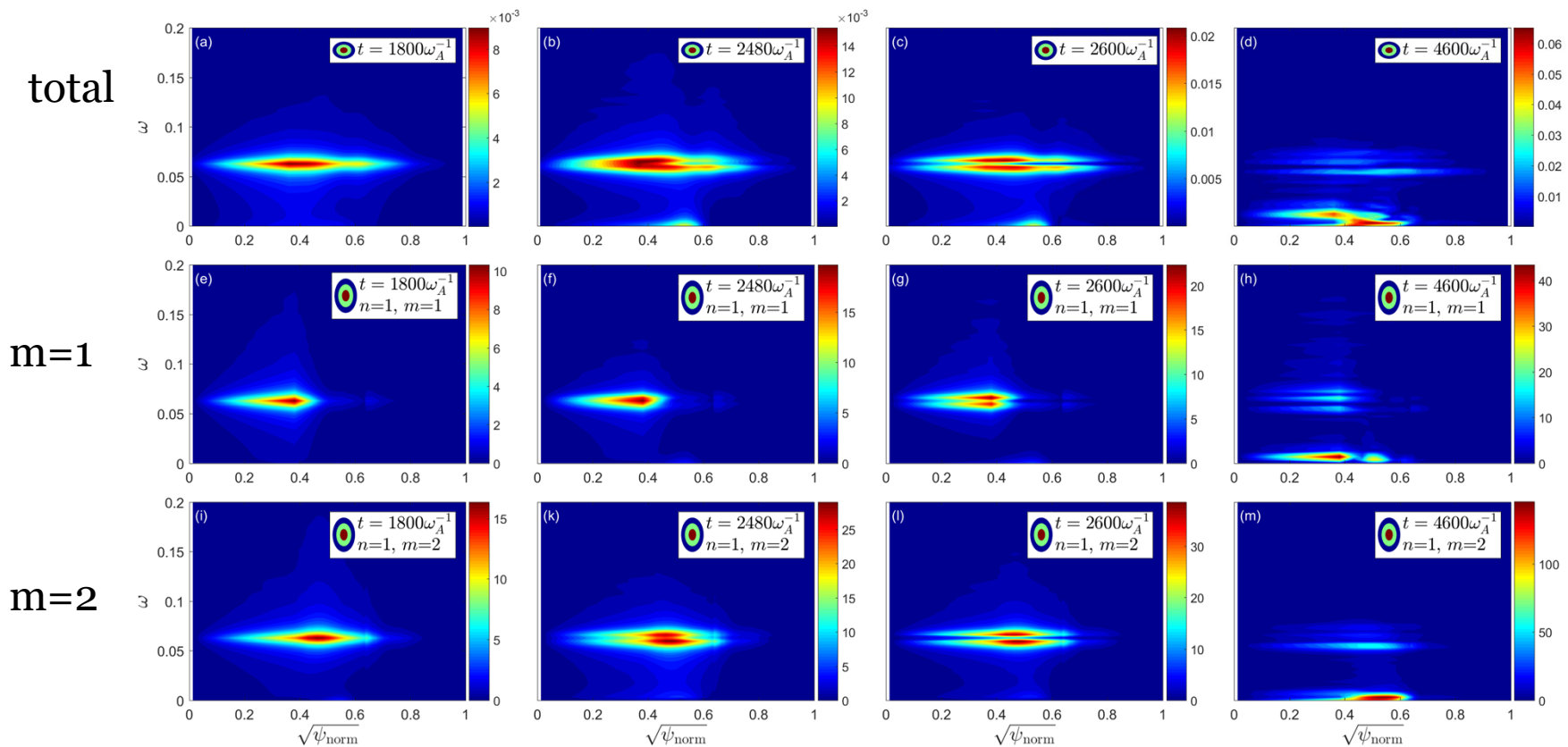
High frequency branch : TAE
Low frequency branch : tearing mode



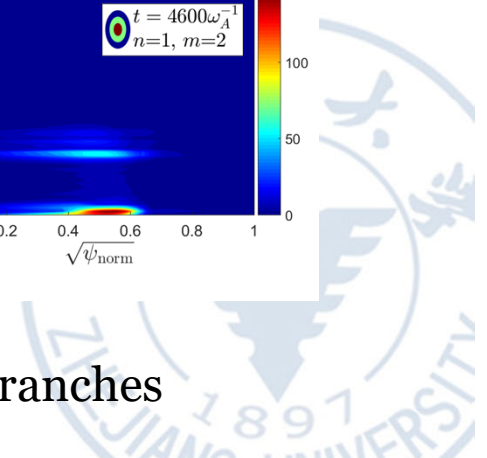
Radial structure of mode power spectrum

TM: low frequency around the $q=2$ rational surface ($r=0.5$)

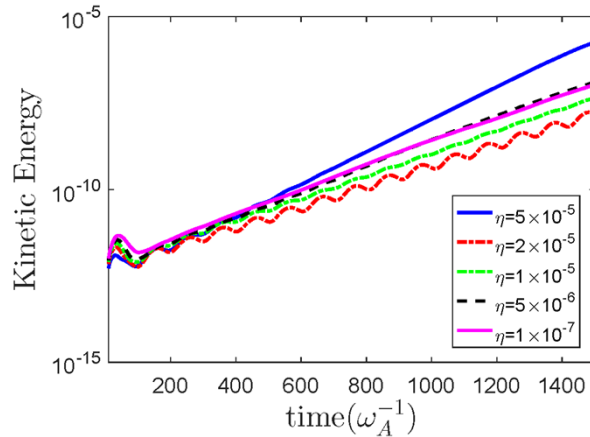
TAE: high frequency peaked near $r=0.4$ and splits into two branches



$m/n=2/1$ poloidal harmonic first split into two branches

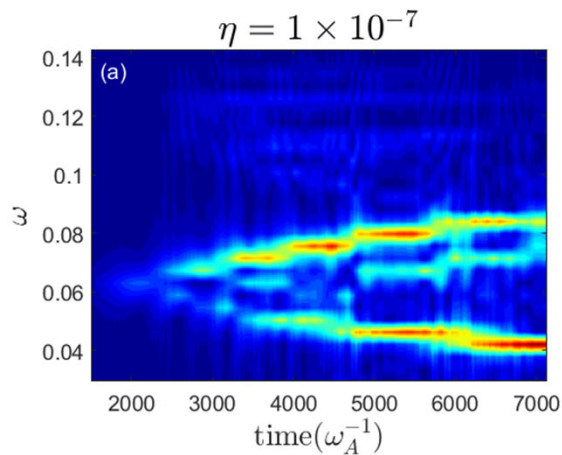


Comparisons for different resistivity

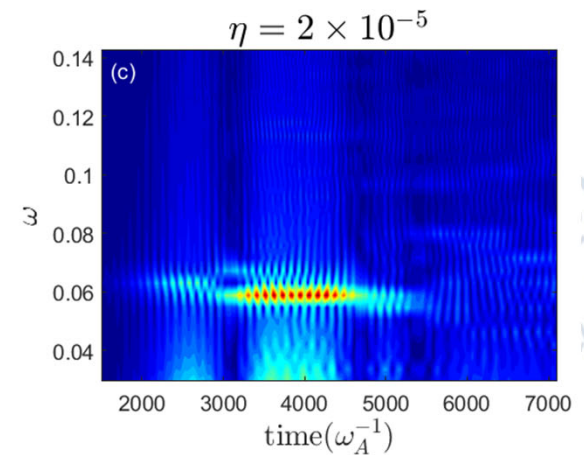
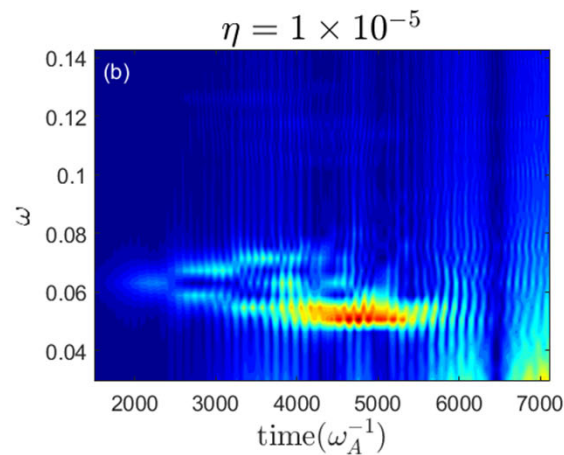


← Linear:
 Small resistivity: damping(TAE)
 Large resistivity: destabilize(tearing mode)

Nonlinear:
 $\eta \uparrow$ frequency chirping \downarrow



weak TM



strong TM

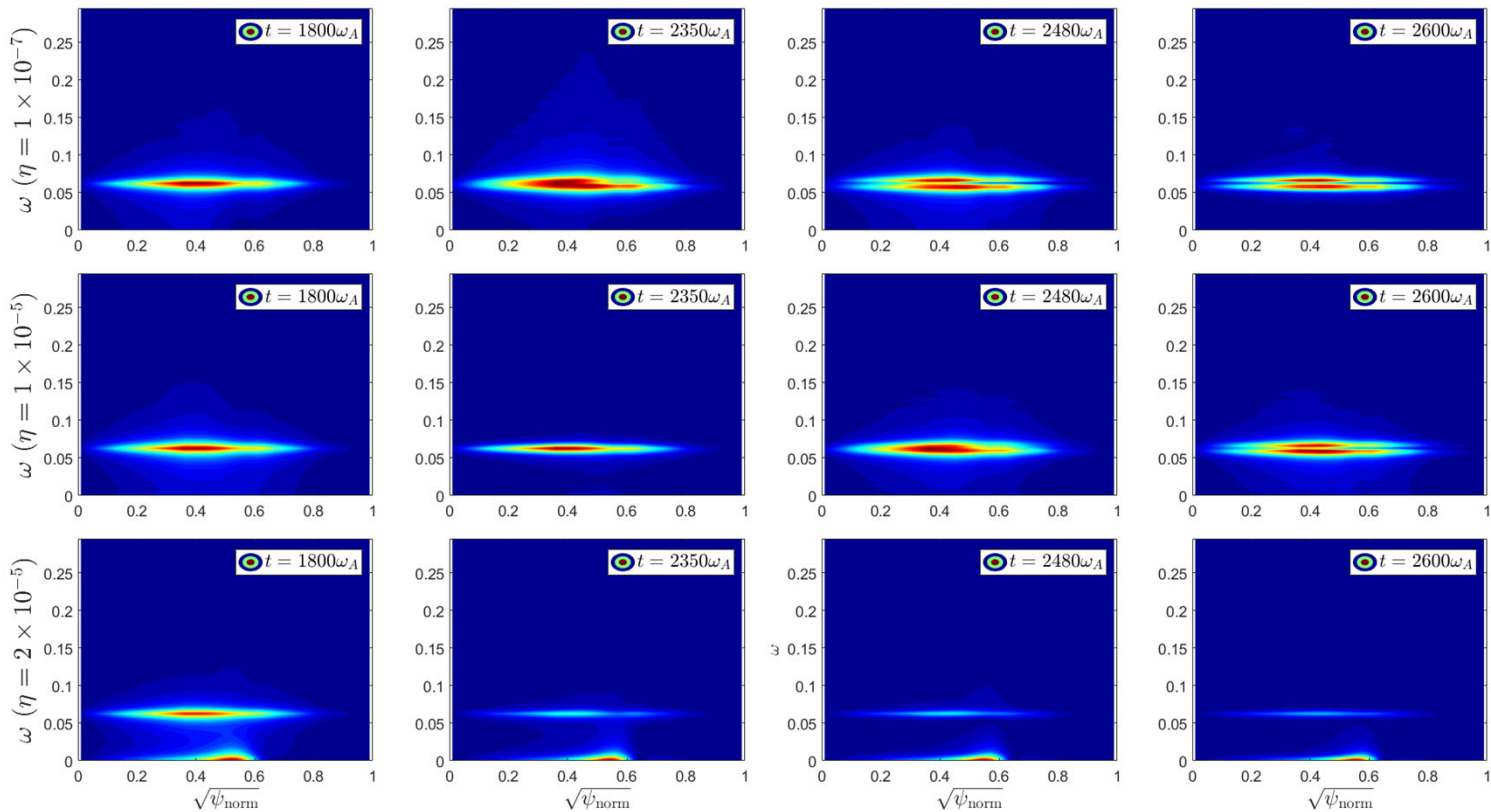




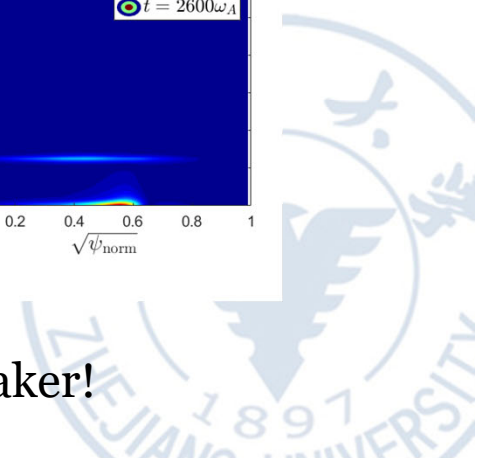
Comparisons of radial frequency structure for different resistivity

Weak
TM

Strong
TM



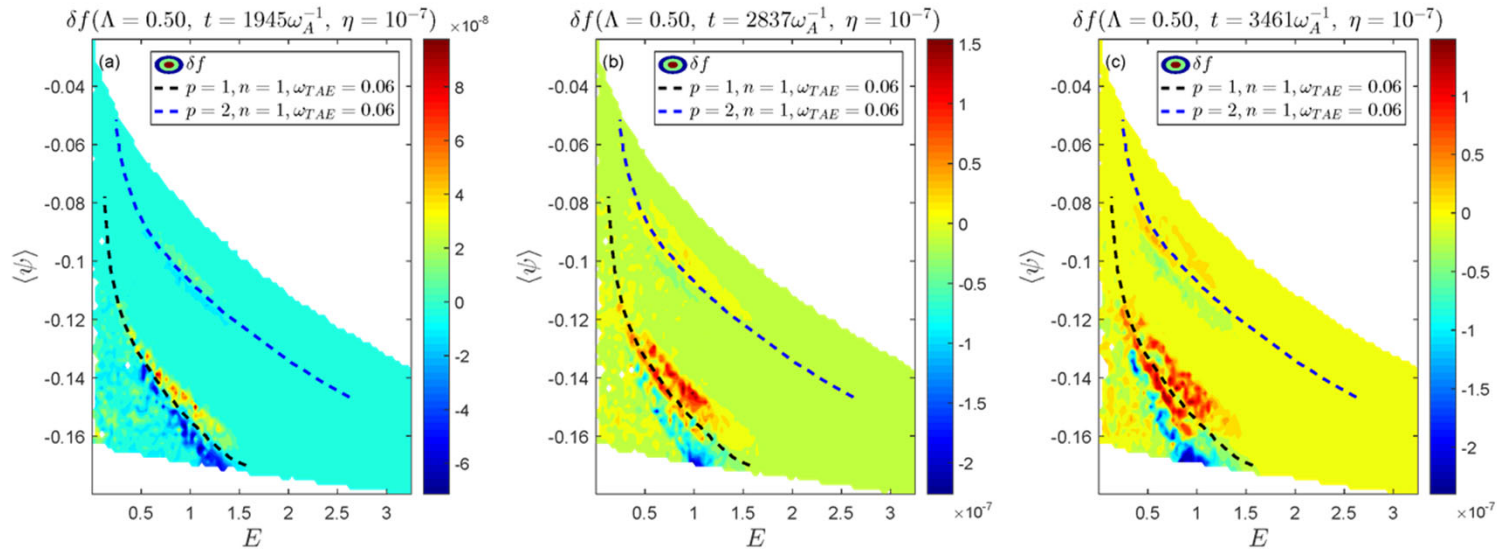
Tearing mode make the frequency chirping weaker!



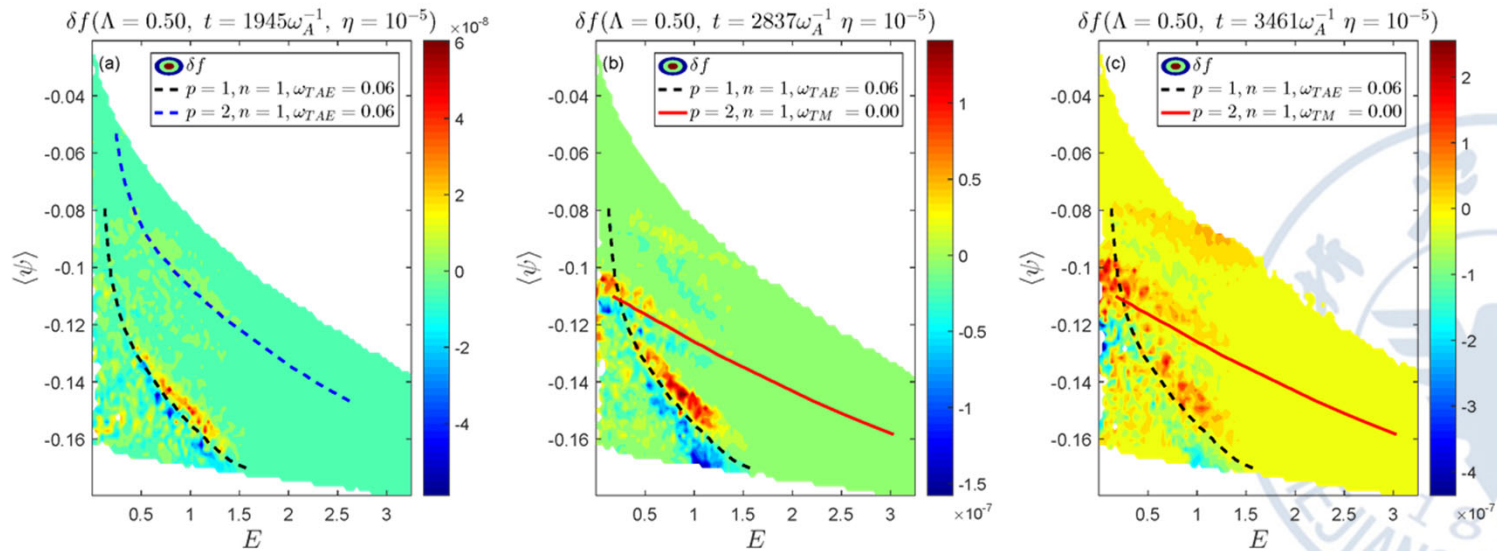


Comparisons of phase space structure for different resistivity for passing particle

$\eta=1e-7$



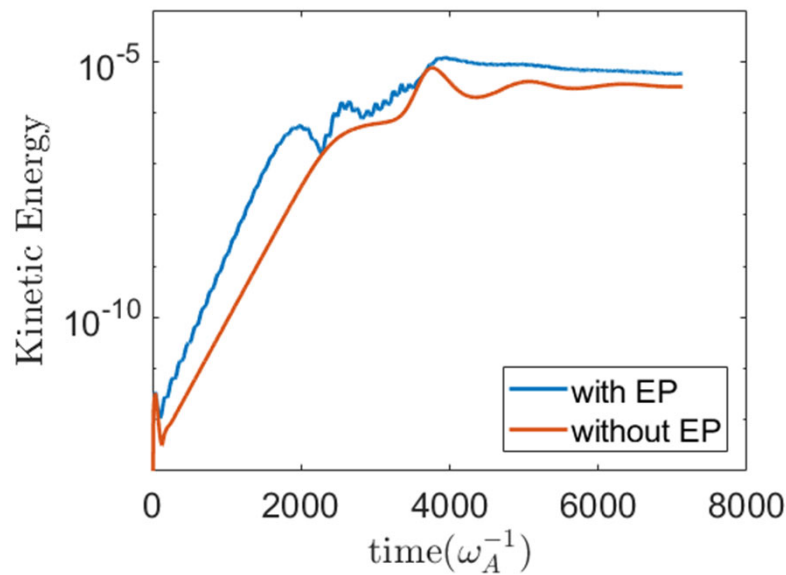
$\eta=1e-5$



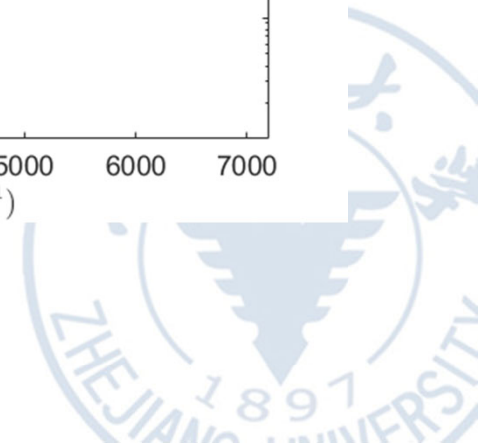
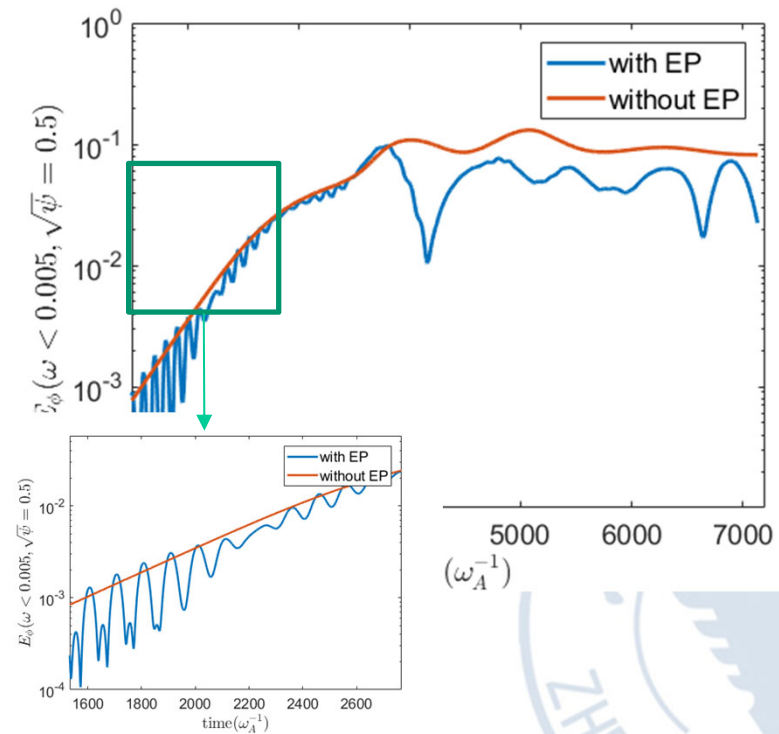
Comparison w/o EP

total ke

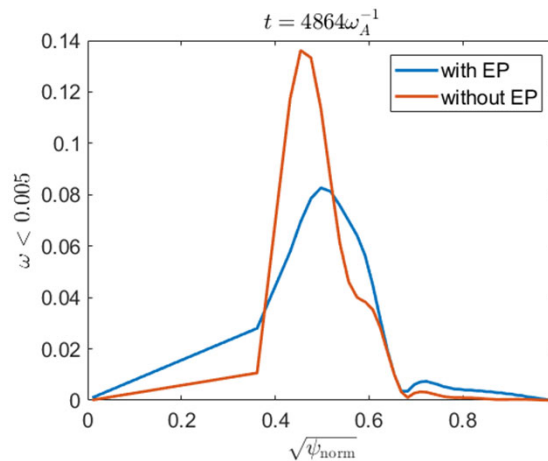
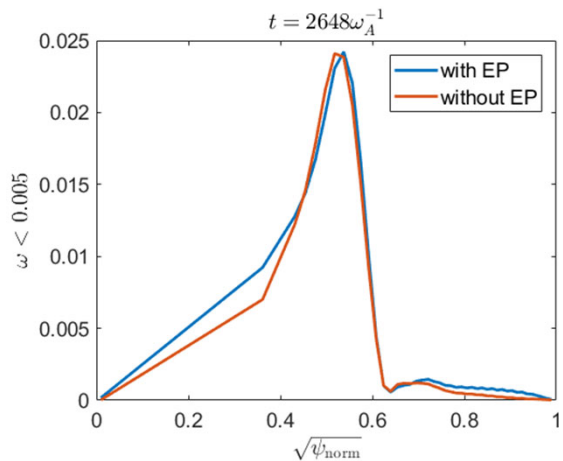
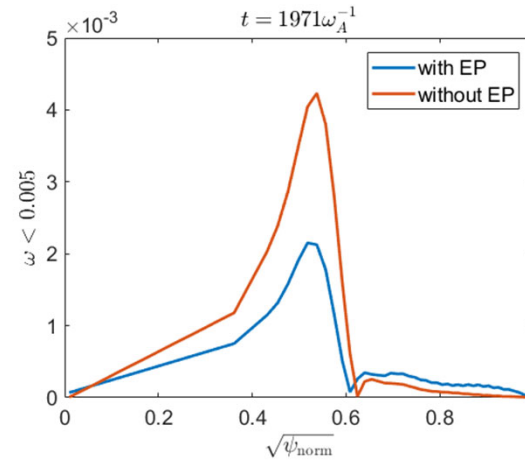
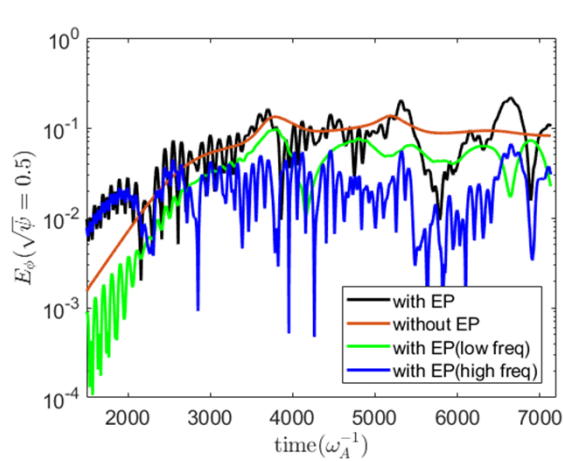
low frequency part of E_ϕ



The low frequency part of E_ϕ is reduced by the TAE



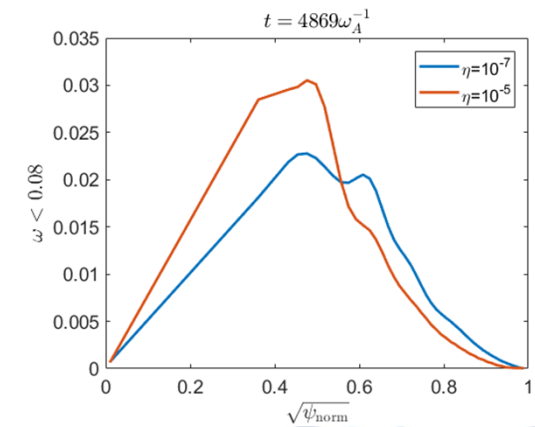
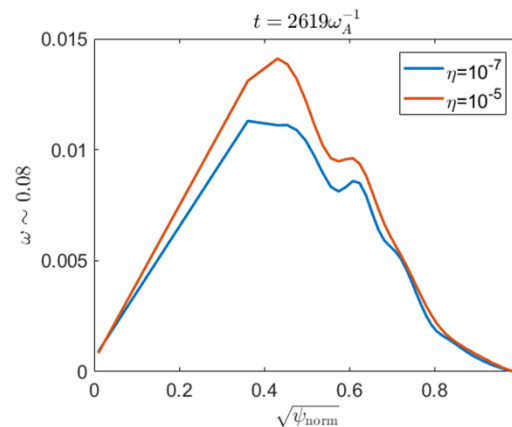
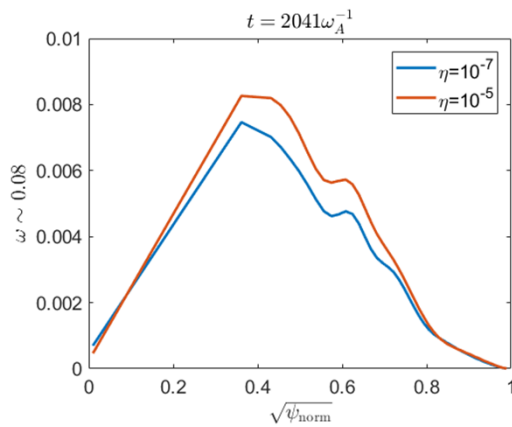
Snapshot of low frequency mode structure



Three figs are correspond to three peaks in evolution of kinetic energy. Here the mode structure is time averaged with $78\omega_A^{-1}$ region



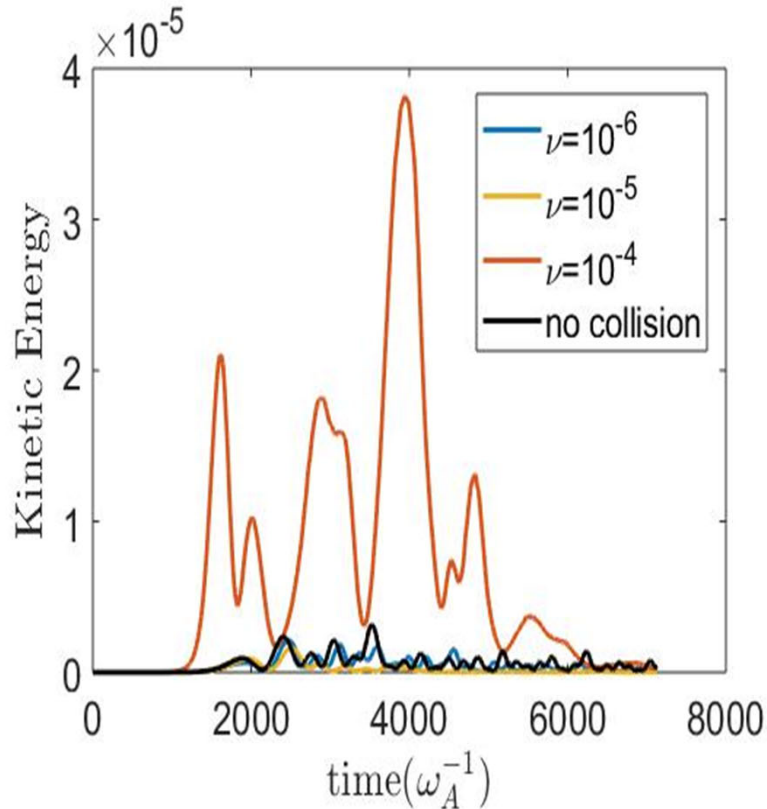
TM effect on TAE



Here
 $\omega = 0.06 \pm 0.02$



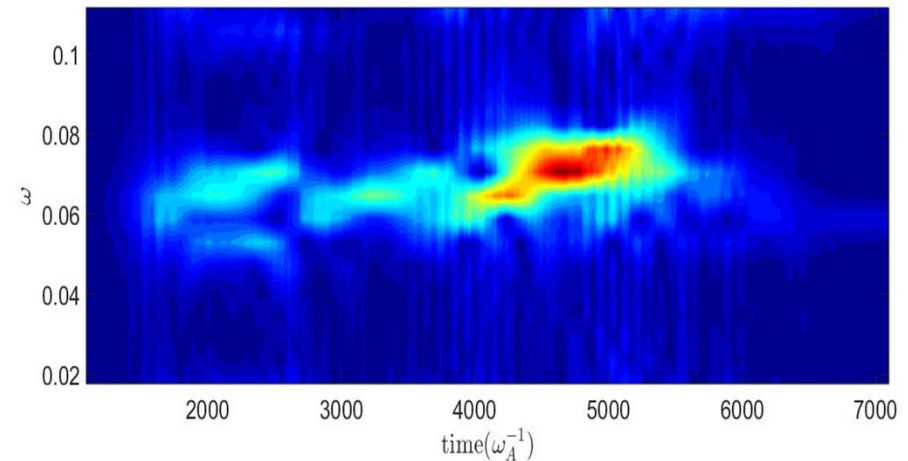
With inclusion of source and sink



TAE re-bursts are observed with increase of collisional frequency.

$$C(f) = \nu_d \frac{\partial}{\partial \lambda} (1 - \lambda^2) \frac{\partial}{\partial \lambda} f + \frac{\nu}{v^2} \frac{\partial}{\partial v} (v^3 + v_c^3) f$$

pitch angle scattering and slowing down are included in the collisional operator

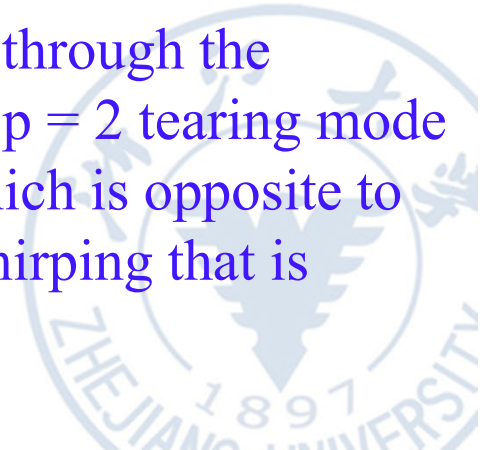


Three successive TAE bursts are detected in the distribution of the power spectrum



4. Brief Summary

- EPM (initially TAE-like or rTAE) is linearly excited.
- During the nonlinear phase, one poloidal component ($m=2$) of EPM remains the frequency unchanged while another poloidal component ($m=3$) of EPM chirps down to a BAE gap. The $m/n=3/2$ mode becomes dominant at the late time
- The $n = 1$ TAE is first excited by isotropic energetic particles at the linear stage and reaches the first steady state due to wave-particle interaction. After the saturation of the $n = 1$ TAE, the $m/n = 2/1$ tearing mode grows continuously and reaches its steady state due to nonlinear mode-mode coupling.
- The enhancement of the tearing mode activity with increase of the resistivity could weaken the TAE frequency chirping through the interaction between the $p = 1$ TAE resonance and the $p = 2$ tearing mode resonance for passing particles in the phase space, which is opposite to the classical physical picture of the TAE frequency chirping that is enhanced with increase of dissipation.





浙江大學
ZHEJIANG UNIVERSITY



Thank you for attention!

